

**Book of Abstracts** 



### 12th International Young Scientist conference

# Developments in Optics and Communications 2016

**Book of Abstracts** 

#### Editor:

#### Martins Bruvelis

Faculty of Physics and Mathematics University of Latvia Zellu street 8, Riga, LV1002, Latvia e-mail: martins.bruvelis@gmail.com URL: https://linkedin.com/in/bruvelis

### Assistant Editor:

Arturs Cinins

Faculty of Physics and Mathematics University of Latvia Zellu street 8, Riga, LV1002, Latvia e-mail: arturs.cinins@gmail.com

URL: https://plus.google.com/+ArtursCinins

### **Assistant Editor:**

Elza Linina

Institute of Solid State Physics University of Latvia 8 Kengaraga street, Riga, LV1063, Latvia

e-mail: elza.linina@gmail.com

URL: https://plus.google.com/105748436706316446820

ISBN: 978-9934-556-02-9 e-ISBN: 978-9934-556-03-6

© 2016 University of Latvia, M. Bruvelis, A. Cinins, E. Linina

This work is subject to copyright. All rights are reserved. This work may not be translated or copied in whole or in part without the written permission of the publisher (University of Latvia, M. Bruvelis, A. Cinins, E. Linina).

Cover design: M. Bruvelis, A. Cinins, E. Linina, Riga

www.docriga.lv

### 1 Welcome

The Organizing Committee kindly welcomes you to the 12th International Young Scientist conference "Developments in Optics and Communications 2016". This conference is organized jointly by University of Latvia SPIE student chapter and OSA Latvian student chapter. The purpose of this conference is to bring together students and young scientists working experimentally and theoretically in the fields of optics and photonics to share and exchange new ideas and to establish contacts for future collaboration. The conference traditionally covers the following topics:

- Laser Physics and Spectroscopy;
- · Biophotonics;
- · Optical Materials and Phenomena;
- · Vision Science.

The organizers wish you a fruitful conference and a pleasant and memorable stay in the capital of Latvia!

### 1.1 OSA-UL Best student presentation prize

We are delighted to announce that OSA-UL Best student presentation prize will be awarded to the best contributed talk and to the best poster presented at the conference. The talk/poster must be produced and presented by a student. The prize jury consists of members of ULSPIE and OSA-UL. The winners of the prize will be announced during the award ceremony at the end of the conference. The prize consists of a diploma and 50€ in cash.

Evaluation criteria for oral and poster presentations are published on the conference web page www.docriga.lv.

### 1.2 The Organizing Committee

#### 1.2.1 DOC chairs

· Artis Brasovs

PhD student

Laboratory of Magnetic Soft Materials, University of Latvia

· Elza Linina

BSc student

Institute of Solid State Physics, University of Latvia

### 1.2.2 Organizers

### Arturs Cinins

PhD student Faculty of Physics and Mathematics, University of Latvia

### · Paula Jankovska

BSc student Institute of Solid State Physics, University of Latvia

### Varis Karitans

Leading researcher Institute Solid State Physics, University of Latvia

#### · Matiss Lacis

MSc student Institute of Biomedical Engineering and Nanotechnologies, Riga Technical university

### · Ilze Oshina

MSc student Institute of Atomic Physics and Spectroscopy, University of Latvia

### · Karola Panke

PhD student Department of Optometry and Vision science, University of Latvia

### Janis Tjarve

BSc student Faculty of Physics and Mathematics, University of Latvia

### 1.2.3 Scientific committee

### · Prof. Ruvin Ferber

Faculty of Physics and Mathematics, University of Latvia

#### Prof. Maris Ozolins

Department of Optometry and Vision science, University of Latvia

### · Prof. Uldis Rogulis

Institute of Solid State Physics, University of Latvia

### · Prof. Janis Spigulis

Institute of Atmoic Physics and Spectroscopy, University of Latvia

### 2 Program

Monday, 21st of March			
8:45 – 9:30	Registration		
9:30 – 10:00	Openi	ng session	
10:00 - 10:10	OPTE	ζ	
10:10 – 10:50	IN01	Invited: Mara Reinfelde	
10:50 – 11:10	A01		
11:10 – 11:30	A02	Laser Physics and Spectroscopy contributed talks	
11:30 – 11:50	A03		
11:50 – 12:30	Lunch		
12:30 – 13:10	IN02	Invited: Florian Gahbauer	
13:10 – 13:20	Short break		
13:20 – 13:40	B01	Optical Materials and Phenomena contributed talks	
13:40 – 14:00	B02	Optical materials and rhenomena contributed tanks	
14:00 – 14:20	Coffee Break		
14:20 – 14:40	B03	Optical Materials and Phenomena contributed talks	
14:40 – 15:00	B04	Optical materials and Phenomena contributed talks	
15:00 – 15:20	B05		
15:20 – 17:00	P	Poster session (LasPhys + OptMat)	

Tuesday, 22nd of March			
9:00 – 9:40	IN03	Invited: Igor Meglinski	
9:40 – 10:00	C01	Biophotonics contributed talks	
10:00 – 10:10	Short	break	
10:10 – 10:30	C02		
10:30 – 10:50	C03	Biophotonics contributed talks	
10:50 – 11:10	C04		
11:10 – 11:20	Short	break	
11:20 – 11:40	D01		
11:40 – 12:00	D02	Vision Science contributed talks	
12:00 – 12:20	D03		
12:20 – 13:00	Lunch		
13:00 – 13:40	IN04	Invited: Zeev Zalevsky	
13:40 – 14:00	D04	Vision Science contributed talks	
14:00 – 14:20	D05	Vision Science contributed tarks	
14:20 – 14:40	Coffee	Break	
14:40 – 16:00	P	Poster session (Bio + Vis)	
16:00 – 16:20	Closin	losing Session	
16:30 –	Tour t	o Old Riga	

### **Detailed Program & Schedule**

1	wei	come		V1
	1.1	OSA-U	L Best student presentation prize	vi
	1.2	The Or	ganizing Committee	vi
		1.2.1	DOC chairs	vi
			Organizers	vii
		1.2.3	Scientific committee	vii
2	Prog	gram		viii
De	etaile	d Progr	ram & Schedule	ix
M	ond	ay, Ma	arch 21, 2016	1
	08:4	15 - 09:3	30 Registration	
	09:3	80 - 10:0	00 Opening session	
	10:0	00 - 10:1	10 ОРТЕК	
(L	asPh	ys) Lase	er physics and spectroscopy	1
	Invi	ted talk	τ	
	10:1		50 <u>Mara Reinfelde</u> al application of holography	1
	10:5		10 <u>Janis Smits</u> volution - a tool for enhanced resolution magnetic images	2
	11:1	0 - 11:	<b>30</b> K. Vaicekonis	
			on spin-relaxation in nitrogen-vacancy centers in diamond	
				3
	11:3		50 <u>A. Erglis</u> n - Back effect in Caesium atoms	4
	11:5		30 Lunch break	
<b>(</b> 0	ptMa	ıt) Opti	cal materials and phenomena	4
•	_	ted talk	-	
			10 Florian Gahbauer	
	14.0		tic sensing with nitrogen-vacancy (NV) centres in synthetic	
		diamo	·	4

13:10	- 13:20	Short break	
I	Infra-red	Kaspars Pudzs radiation sensors based on thermoelectric effect of orfilms	6
I	Molecule	Raitis Grzibovskis ionization energy and morphology dependence on film of two indandione derivatives	7
14:00	- 14:20	Coffee break	
I	Preparatio	Julija Pervenecka on of microstructure and amplified spontaneous emistraniliden derivative containing SU-8 films	8
		Jelena Mikelsone lographic recording in azo-epoxy polymer films	9
		Arturs Bundulis ation of two-photon absorption and Kerr effect of or-	
		rerials by z-scan method	10
8	ganic mat		10 11
Poster se	ganic mat ession (La	rerials by z-scan method	
Poster se 15:40	ession (La ) - 17:00 Inga Bric Measurem	erials by z-scan method	
Poster se 15:40 P01 F1	ession (La 0 - 17:00 Inga Bric Measurem frequency D.N. Mer Ab initio r	rerials by z-scan method	11
Poster se 15:40 P01 P02 P02 P04	ession (La ) - 17:00 Inga Bric Measurem frequency D.N. Mer Ab initio r low-lying Aija Grar	rerials by z-scan method	<b>11</b> 11
Poster se 15:40 P01 P02 P04 P04 P05	ession (La 0 - 17:00 Inga Bric Measuren frequency D.N. Mer Ab initio r low-lying Aija Grar High-reso Aija Grar Analysis a	rerials by z-scan method	<b>11</b> 11 12

P0/	Luminescence of europium and dysprosium co-doped oxyfluoride glasses	16
P08	Mārcis Greiselis Spectroscopic study of the bright star HD179821	17
P09	Reinis Lazda Modeling of Optically detectable magnetic resonances of nitrogen - vacancy optical centers in diamond crystal	18
P10	Janis Smits Deconvolution - a tool for enhanced resolution magnetic images	19
P11	Edgars Butanovs Photoluminescence in 2D transition metal dichalcogenide nanostructures	20
P12	Andris Antuzevics Structure of $Gd^{3+}$ ions in oxyfluoride glass ceramics containing fluorite crystallites	21
P13	Meldra Kemere Luminescence and quantum efficiency of europium doped oxyfluoride glasses and glass-ceramics	22
P15	<u>Igors Mihailovs</u> Modelling second-order optical non-linearity of organic material through simple quantum chemical calculations	23
P16	$\frac{\text{Girts Zageris}}{\text{Pr}^{3+} \text{ luminescence in oxyfluriode glass and oxyfluoride glass ceramic containing NaLaF}_4 \dots \dots$	24
Tuesd	ay, March 22, 2016	25
(Bio) Bi	iophotonics	25
	ted talk 0 - 09:40 <u>Igor Meglinski</u> Cloud Monte Carlo for the needs of biomedical optics	25
09:4	O - 10:00 Gatis Tunens  Modeling skin diffuse reflectance spectra in the near-infrared and visible spectral range	26

10:00 - 10:10 Snort break	
10:10 - 10:30 <u>Aleksandrs Leitis</u> Selective Plane Illumination Microscope Using Non-Spreading Airy Beams	27
10:30 - 10:50 <u>Lisa Kobayashi Frisk</u> Diffuse Reflectance Spectroscopy for evaluation of tissue chromophore composition	28
10:50 - 11:10 <u>Ilze Oshina</u> Mapping of skin chromophores by snapshot taken with a smartphone	29
11:10 - 11:20 Short break	
(Vis) Vision Science	30
11:20 - 11:40 Olga Danilenko The compound mechanism of adaptation to high contrast	30
11:40 - 12:00 Sanita Liduma  The impact of position of corneal apex in keratoconus on visual acuity and contrast sensitivity	31
12:00 - 12:20 <u>Ilze Laicane</u> Biological motion processing in central and peripheral visual field	32
12:20 - 13:00 Lunch break	
Invited talk  13:00 - 13:40 Zeev Zalevsky  Super resolved and extended depth of focus concepts for remote and ophthalmic imaging systems	33
13:40 - 14:00 <u>Varis Karitans</u> Manually tunable lens based eye model	34
14:00 - 14:20 <u>Sergejs Fomins</u> Seasonal environmental spectrophotometry	35
14:20 - 14:40 Coffee break	
Poster session (Bio+Vis)	36
14:40 - 16:00 Poster session (Bio + Vis)	

Р17	Antra Dzerve Investigation of photon time-of-flight in human skin	36
P18	Reinis Janovskis Infrared spectroscopy and imaging for estimation of skin hydration	37
P19	<u>Liene Zarina</u> Figure recognition time in mental rotation task according to their size	38
P20	Sabine Matulevica Gender differences in mental rotation test	39
P21	Annija Gulbe Handedness differences in mental rotation task	40
P22	<u>Lelde Zabere</u> Color vision resolution assessment for sorting and forced choice methods	41
P23	$\frac{Elina\ Vevere}{Spatial\ speeded\ verification\ test\ in\ condition\ of\ mental\ fatigue.}$	42
P24	Anete Petrova Changes of blur sensitivity during the day	43
P25	Karola Panke Changes in physiological astigmatism with accommodation in emmetropes	44
P26	Julija Tomilova Pupil diameter changes within mental rotation task under fatigue conditions	45
P27	K. Shavanova The possibility of using NnO NPs as a transducer for optical biosensor for the blv leucosis detection	46
P28	Yuliia Ruban Estimation of the effect of radionuclide contamination on vicia sativa l. cfi parameters using "floratest" optical biosensor	47
P29	Nelya Shpyrka Control of patulin by immune biosensor based on the structured nano-porouse silicon	48

P30 Ingrida Lavrinovica	
Evaluation of effective area of ytterbium doped optical fiber	49
P31 Kalvis Kudrats	
Device for retinal illumination and circadian light monitoring .	50
Closing Session	51
16:00 - 16:30 Closing Session	
10.00 - 10.00 Glosing Session	
Tour to Old Riga	51
·	01
16:30 Tour to Old Riga	
Notes	51

### Practical application of holography

Mara Reinfelde Institute of Solid State Physics, University of Latvia, 8 Kengaraga str., Riga, LV-1063, Latvia

Since the discovery the principles of holography are used in a wide variety of fields of science, technique and everyday life. Physical principles of holography are based on processes related with nature of wave-like phenomenon – interference and diffraction. Hologram is the pattern of interference fixed in a certain space area and formed by flux of coherent waves coming from the same source. Non-disturbed part of that flux operates as frame of reference (reference wave), meanwhile other part bring the corrections reflected from the object (object wave). Thus the hologram can be considered as the code describing the given object. When the object is moved away, the reference wave by diffraction on hologram will create the precise image of the object.

In broader sense the methods of holography has been applied to such fields as Xray spectroscopy, electron microscopy, and acoustics and even in attempts to explain the structure of the Universe. Nevertheless the more profound theoretical as well as practical part of holography relates to visible spectral range of electromagnetic waves  $(400-800 \ nm)$  and we are talking about optical holography. From the historical point of view the basic principles of holography were developed by D. Gabor in 1947, but first 3-dimensional holographic images were realized at 60-ies of previous century by E. Leith and J. Upatnieks in USA and by Yu. Denisjuk in Russia. There where the burst of inventions, attempts and speculations in 70-ies how and where ideas of holography could be utilized. But the development of science and technology as well the market demands highlighted the priority branches where choices of holography could be used. Nowadays our society more or less is familiar with three-dimensional display holograms as art works and real copies for treasures of museum. The widespread public use and industrial importance is gained embossed holograms - multiple repeating of so called master hologram by printing on thermoplastic material. With the development of communication systems the demands are increasing for holographic optical elements (HOE).

For every type of hologram the key condition of desirable quality is the recording material. Some of the characteristics required are high photosensitivity, resolution and low price. Accordingly, the investigation and creating of new classes of materials is carried out. There are some centres in Latvia practicing holography and holographic methods for studies of light sensitive materials. In the Institute of Solid State Physics and Riga Technical University there are worked on organic materials and amorphous chalcogenides, in Daugavpils University the new holographic technologies is being developed.

# Deconvolution - a tool for enhanced resolution magnetic images

Janis Smits<sup>1</sup>, Florian Gahbauer<sup>1</sup>, Andris Berzins<sup>1</sup>, Kaspars Erglis<sup>2</sup>

<sup>1</sup>Laser Centre, University of Latvia, Zellu street 25, Riga, Latvia, LV-1002

<sup>2</sup> MMML Lab, Faculty of Physics and Mathematics, University of Latvia, Riga, LV-1002, Latvia

\*E-mail: smitsjanis@gmail.com,

Nitrogen vacancy (NV) centers in diamond have shown great promise for magnetic field measurements and have recently been used to to image magnetic field distributions in biological systems [1]. However as the scale of observed fields reaches that of optical wavelengths, optical resolution poses a problem for obtaining high quality magnetic images.

In this work the possibility of using deconvolution methods to enhance the resolution of magnetic images was examined. A forward problem was solved assuming ideal dipoles and various distances from NV centers. Two deconvolution algorithms were examined (the Wiener filter and Richardson-Lucy deconvolution), examining their behavior with different noise and blurring kernels applied to the images. Finally the effect of depth density distribution of NV centers is incorporated in the model. The forward problem consists of obtaining the real magnetic field of an ideal dipole, generating Lorentz distributions with an expectation value that matches the magnetic field, blurring the image by discrete convolution and applying Poisson noise.

### Ackowledgements

This study was supported by the M-ERA.NET project MyND no. Z/15/1366.

#### References

[1] D. Le Sage, K. Arai, D. R. Glenn, S. J. DeVience, L. M. Pham, L. Rahn-Lee, M. D. Lukin, A. Yacoby, A. Komeili, and R. L. Walsworth, Nature **496**, 486 (2013).

### Electron spin-relaxation in nitrogen-vacancy centers in diamond lattice

A. Jarmola<sup>1</sup>, A. Berzins<sup>1</sup>, J. Smits<sup>1</sup>, K. Smits<sup>2</sup>, J. Prikulis<sup>3</sup>, F. Gahbauer<sup>1</sup>, R. Ferber<sup>1</sup>, D. Erts<sup>3</sup>, M. Auzinsh<sup>1</sup>, D. Budker<sup>4,5</sup>, K. Vaicekonis<sup>1,\*</sup>

<sup>1</sup>Laser Centre, University of Latvia, Rainis blvd. 19, Riga, Latvia <sup>2</sup>Institute of Solid State Physics, University of Latvia, 8 Kengaraga Street, Riga, Latvia <sup>3</sup>Institute of Chemical Physics, University of Latvia, 19 Rainis Blvd., Riga, Latvia <sup>4</sup>Helmholtz-Institut Mainz, Johannes Gutenberg Universitat Mainz, Germany <sup>5</sup>Department of Physics, University of California, Berkeley, California, USA \*E-mail: karlisvaicekonis@gmail.com,

Nitrogen-vacancy (NV) centers in diamond can be used to analyse electron spins, external magnetic fields and temperature on molecular scale and to detect low concentration paramagnetic molecules and ions, but to do that, there is a need to understand fundamental interactions that can interfere with the precision of measurements.

One way to explore these interactions is by using  $T_1$  (longitudinal spin-relaxation) time measurements, that represents interactions between NV center and diamond lattice, impurities, and other NV centers. We present time dependence on concentration of nitrogen-vacancy centers in diamonds and on magnetic field [1]. Figure 1 shows an example of such a dependence. Our sample has small regions of NV centers where each region has different concentration of NV centers. We can determine the relaxation rates by analyzing the magnetic field and concentration dependent fluorescence signals acquired by using a laser light and microwave (MW) pulse sequence. The basic principle of the experiment is as follows: With a green laser light pulse we pump NV centers into  $m_s = 0$  level, after which we block laser light and radiate the sample with MW to transfer the population to the  $m_s = \pm 1$  level, then it gets illuminated again to probe the population distribution. This process is repeated by using variable intervals between laser pulses also with and without microwaves to cancel out noise.

The Riga group gratefully acknowledges financial support from the Latvian State Research Programme (VPP) project IMIS<sup>2</sup>.

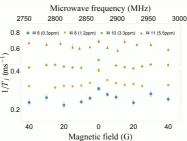


Figure 1:  $1/T_1$  time dependence on Magnetic field and concentration.

#### References

[1] A. Jarmola, APPLIED PHYSICS LETTERS 107, 242403 (2015)

### Paschen - Back effect in Caesium atoms

Andris Erglis<sup>1,\*</sup>, Marcis Auzinsh<sup>1</sup>, Andris Berzins<sup>1</sup>, Ruvins Ferbers<sup>1</sup>, Janis Smits<sup>1</sup>, <sup>1</sup>Laser

Centre, University of Latvia, Rainis blvd. 19, Riga, Latvia, LV-1586

\*E-mail:andris.erglis@fizmati.lv

Alkali metal atoms have great potential to demonstrate fundamental interactions between atoms and the magnetic field. We want to present didactic material with clear and demonstrative graphs, in which we can see obvious energy level splitting of Caesium. These effects can be also used to measure the magnetic field in a wide range of the magnetic field values.

We present experimental and theoretical research of Paschen-Back effect in Caesium  $D_1$  and  $D_2$  lines. For absorption measurements it is enough to use a diode laser with low output power (approximately 2  $\mu$ W), that can be appealing for multiple applications. To split hyperfine energy levels of Caesium, we use an electromagnet which produces homogeneous magnetic field within the range of one tesla.

We use two types of excitation ( $\sigma$  and  $\pi$ ).  $\sigma$  excitation happens, when polarized light direction is perpendicular to the magnetic field lines, but  $\pi$  excitation happens, when they are parallel.

In Figure 1 one can see both cases: a)  $\pi$  excitation and b)  $\sigma$  excitation.

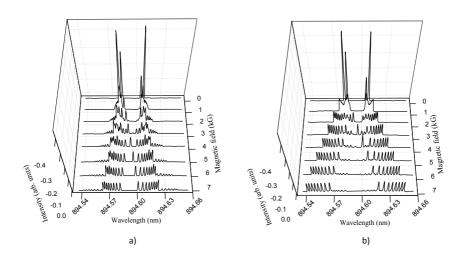


Figure 2: a)  $\pi$  excitation; b)  $\sigma$  excitation.

### Acknowledgments

We gratefully acknowledge Latvian Council of Science project Nr. 119/2012 for financial support.

# Magnetic sensing with nitrogen-vacancy (NV) centres in synthetic diamond

### Dr. Florian Gahbauer Laser Centre, University of Latvia, Riga, Latvia E-mail: florian.gahbauer@lu.lv

Nitrogen-vacancy (NV) centres are defects created in a diamond lattice when a carbon atom adjacent to a vacancy is replaced by a nitrogen atom. The defect has an energy level structure with a triplet ground state with properties that allow it to be manipulated by the interaction of light, microwave radiation, and magnetic fields. One of the features that makes them particularly attractive for sensing and quantum information applications is that the ground state can be polarised by illuminating the defect with green light and the intensity of red fluorescence depends on the polarisation state. The coherence time is long for solid state systems, and at the same time, it is possible to address a single NV centre for maximum spatial resolution or an ensemble of NV centres for maximum magnetic field sensitivity. We will discuss the physics behind NV centres and their application to magnetic field measurement, in particular to magnetic field imaging based on optically detected magnetic resonance and detection of small magnetic dipoles based on measurements of the longitudinal relaxation rate.

# Infra-red radiation sensors based on thermoelectric effect of organic thin films

### Kaspars Pudzs

Institute of Solid State Physics, Kengaraga 8, Riga, Latvia, LV-1063 \*E-mail: kaspars.pudzs@cfi.lu.lv,

With the development of modern technology, there is an increasing need for effective, high-speed and low-cost infra-red sensors. Inorganic materials, that are used most commonly, have a relatively high thermal conductivity, which prevents their use in thin films. These materials are also more effective at high temperatures, and their availability is limited, which raises the cost of these sensors.

Organic materials have high Seebeck coefficient values, that can reach 1.8~mV/K [1-3]. Due to their properties, thin films of such materials can be used in thermoelectric (TE) sensors, such as sensors for the determination of laser beam position.

One of the organic material classes, that could potentially be used in sensors, is a metal phthalocyanine. So far, the metal phthalocyanines (MePc) have been studied intensively for gas sensor applications. Recent theoretical calculations show that MePc could be potentially used as TE materials in the aforementioned applications. ZT factor for N-doped nickel phthalocyanine mono-crystal can reach up to 2.5. Growing a clean, perfect single crystal is a very slow and complicated process, which would hinder the practical applications of this material. Therefore, the aim of this work is to study the TE properties of organic polycrystalline thin films, obtained by thermal evaporation in vacuum. From a wide range of organic materials, the emphasis is put on MePc and cyclic hydrocarbons (namely tetrathiotetracene), because these materials are stable, and previous studies have shown the potential applications in TE converters.

Impact of preparation conditions on film morphology as well as electrical and TE properties of obtained thin films were studied. Scanning Electron Microscopy was used to investigate the morphology of these films. Electrical conductivity up to 2 S/cm was measured using the four probe technique. The values of Seebeck coefficient in thin film plane and perpendicular to the film were measured by a custom-made setup.

Financial support provided by Scientific Research Project for Students and Young Researchers No. SJZ2015/13 realized at the Institute of Solid State Physics, University of Latvia is greatly acknowledged.

- [1] Y. Lin, Z. Shi, and P. L. D. Wildfong, J. Pharm. Biomed. Anal. 51, 979-984 (2010)
- [2] G. S. Nolas, J. Sharp, and H. J. Goldsmid, *Thermoelectrics: Basic Principles and New Materials Developments* (pringer-Verlag, Berlin-Heidelberg-New-York 2001)
- [3] C. Hamann, Phys. Status Solidi, **20**, 481-491 (1967)

## Molecule ionization energy and morphology dependence on film thickness of two indandione derivatives

Raitis Grzibovskis<sup>1,\*</sup>, Aivars Vembris<sup>1</sup>, Kaspars Pudzs<sup>1</sup>
<sup>1</sup>Institute of Solid State Physics, Kengaraga 8, Riga, Latvia, LV-1063
\*E-mail: raitis.g@cfi.lu.lv,

Nowadays most organic devices as organic light emitting diodes (OLEDs) or organic solar cells consist of layers with thickness below 100nm. Information about the morphology and energy levels of thin films at such thickness is essential as the surface and interface effects can appear. In this work we have investigated 2-(4-[N,N-dimethylamino]-benzylidene)-indene-1,3-dione (DMABI) and 2-(4-(bis(2-(trityloxy) ethyl) amino) benzylidene) -2H-indene-1,3-dione (DMABI-6Ph) thin films. DMABI-6Ph is the same DMABI molecule with attached bulky groups which help to form amorphous films from the solutions. DMABI thin films prepared by the thermal evaporation in vacuum were polycrystalline while DMABI-6Ph films made by the spin-coating method were amorphous. SEM images revealed that separate crystals or islands where formed when the thickness of the samples was below 100nm. Photoemission yield spectroscopy was used to determine the ionization energy of the studied compounds. A vacuum level shift as well as ionization energy shift of organic compounds was obtained. Results of ionization energy dependence on film thickness will be presented.

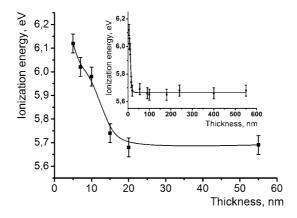


Figure 3: DMABI-6Ph ionization energy dependence on photon energy

# Preparation of microstructure and amplified spontaneous emission in piraniliden derivative containing SU-8 films

Julija Pervenecka\*, Aivars Vembris, Edgars Nitiss, Elza Linina Institute of Solid State Physics, Kengaraga 8, Riga, Latvia, LV-1063
\*E-mail: julija.pervenecka@inbox.lv,

Solid-state laser consist from laser active medium and resonator. Vertical Fabry-Perot microcavity, microring resonator, microdisk resonator and Planar Fabry-Perot waveguide are the most common used resonators in organic semiconductor lasers [1].

DWK-1TB was shown as perspective compound as laser dye in organic solid-state laser. Active medium was obtained by mixing DWK derivatives in a variety of polymers (PMMA (Poly (methyl methacrylate)) and PVK (poly- (N-vinyl carbazole)) matrices) [2], [3].

In this work amplified spontaneous emission and microstructure formation in DWK-1TB/SU-8 systems was investigated. SU-8 was chosen due to their high refraction index and possibility to apply optical lithography method.

Both DWK-1TB and SU-8 compounds were dissolved in GBL (Gamma-Butyrolactone). Solutions were mixed at necessary ration and spin-coated on the glass substrate. Part of the samples was exposed to UV light afterwards. Intensity of UV light was chosen the same as used in lithography.

Amplified spontaneous emission (ASE) measurements were made for both types of the samples to test UV light influence on ASE. Ekspla 310 series laser at 532 nm with repetition rate 10Hz and pulse duration 10 ns was used as light source for ASE measurements. The irradiation area on surface of the sample was stripe form with dimension 3x0.4 mm<sup>2</sup>. Light emission was measured at the edge of the sample.

Microstructures of DWK-1TB/SU-8 films were made by optical lithography. Necessary microstructures in the thin film were recorded by lithography equipment HEIDELBERG instruments  $\mu \rm PG$  101. Record was made with UV diode laser source at 375 nm, with 60 mW power.

In this work formation of SU-8/ DWK-1TB microstructure by lithography and results of amplified spontaneous emission will be discussed.

### Acknowledgment:

This work was supported by National Research program "MultIfunctional Materials and composites, photonics and nanotechnology" (IMIS2)

- [1] Sebastien Forget, Sebastien Chenais, "Organic Solid-State Lasers", Springer-Verlag Berlin Heidelberg 2013, Volume 175, p. 179
- [2] A.Vembris, I.Muzikante, V.Gulbinas, R.Karpicz, G.Sliauzys, A.Miasojedovas, S.Jursenas, Fluorescence and amplified spontaneous emission properties of glass forming styryl-4H-pyran-4-ylidene fragment containing derivatives, Journal of Luminescence, 132, No 9, 2012, pp 2421–2426, doi: 10.1016/j.jlumin.2012.03.063
- [3] Aivars Vembris, Elmars Zarins, Valdis Kokars, Solid state solvation effect and reduced amplified spontaneousemission threshold value of glass forming DCM derivative in PMMA films, Journal of Luminescence 158 (2015) pp 441–446

### Direct holographic recording in azo-epoxy polymer films

<u>Jelena Mikelsone</u>, Janis Teteris Institute of Solid State Physics, Kengaraga 8, Riga, Latvia, LV-1063 E-mail: jelena.mikelsone@gmail.com,

Under the light illumination in azo-compound optical anisotropy is produced. It can lead to surface relief formation due to mass transport. This phenomenon can be used in diffractive optical elements (DOE) production [1,2]. In this work preparation of azo-epoxy polymer resist is presented. Synthesis of such polymer is simple and cheap, environmental friendly solutions in preparation process are used. In result we obtain polymer with low polymerization index, thus surface relief formation will not be inhibited. We studied surface relief formation in azo-epoxy polymers during direct holographic recording. Recording parameters and resists preparation methods were varied and their influence on surface relief formation was studied. We studied recorded surface reliefs by AFM In obtained resists we observed rapid surface relief formation and it's great modulation. Based on obtained results we can conclude azo-epoxy film can be successfully used for DOE production.

#### References

[1]Leonid M. Goldenberg, Lazar Kulikovsky, Olga Kulikovska and Joachim Stumpe, Journal of Materials Chemistry, 19, 6103-6105 (2009)

[2] Leonid M. Goldenberg, Lazar Kulikovsky, Olga Kulikovska and Joachim Stumpe, Journal of Materials Chemistry, 19, 6103-6105 (2009)

# Determination of two-photon absorption and Kerr effect of organic materials by z-scan method

<u>Arturs Bundulis</u>\*, Edgars Nitiss, Janis Busenbergs, Martins Rutkis Institute of Solid State Physics, Kengaraga 8, Riga, Latvia, LV-1063 \*E-mail: bundulis.arturs@gmail.com,

The rapid development of optical technologies for telecommunications sector has created a growing interest on the usage of organic materials in opto-optical devices. Implementation of such devices into practice requires a better understanding of non-linear optical (NLO) effects of organic molecules. Examples include two-photon absorption and Kerr effect, which must be taken into account when designing equipment for optical signal modeling, data storage and power controlling. To determine the optical Kerr coefficient and the two-photon absorption coefficient the "z-scan" method was implemented. Due to this methods simplicity and precision, it is one of the most popular methods for third-order NLO effect analysis.

Thermal lensing effects must be taken into account while carrying out "z-scan" method using nanosecond-pulse laser. For accurate NLO effect analysis picosecond-pulse laser was used in this work.

In this study we will analyze two-photon absorption and Kerr effect of dimethilaminobenziliden-1,3-indandions (DMABI) various derivatives and their application for optical limiting.

The financial support provided by Scientific Research Project for Students and Young Researchers Nr. SJZ2015/16 realized at the Institute of Solid State Physics, University of Latvia is greatly acknowledged.

# Measurements of Rb 5S-5P Transition with a femtosecond optical frequency comb

Inga Brice\*, Janis Alnis, Jazeps Rutkis
Institute of Atomic Physics and Spectroscopy, Skunu iela 4, Riga, Latvia
University of Latvia, Raina Bulvaris 19, Riga, Latvia, LV-1586

\*E-mail: inga02@inbox.lv,

The femtosecond laser frequency comb spectrum is composed of many thousands equidistantly spaced modes. One could simply imagine it as a ruler consisting of narrow modes at known optical frequencies. It has provided us with optical clocks which use optical frequency standards and a clock operating at a higher frequency is more precise.

The advent of precision femtosecond optical combs brings a new set of tools for precision atomic and molecular spectroscopy. For example, it can be used for precision spectroscopy of electronic transitions [1]. The absolute frequency can be determined by the knowledge of frequency rate, offset frequency and a beat note frequency. Additionally, the frequency combs cover a broad spectral interval allowing spectroscopy of different atomic or molecular systems to be done using the same laser system.

We use Erbium fiber based optical frequency comb synthesizer that covers a broad optical spectrum 530...1000 nm emitting 150 fs pulses with 250 MHz repetition frequency. The broad emission spectrum of the frequency comb laser makes it a robust tool Together with a 780 nm ECFL diode laser and a Rb vapor saturation setup we are attempting to measure the hyperfine splitting of Rb atoms.

The laser was slowly scanned across all the Rubidium saturation peaks to calculate the frequency. Using the optical frequencies of the Rubidium peaks, hyperfine splitting constants A and B were also calculated, because these constants can be found in literature and can be used for comparing.

#### References

[1] Th. Udem et al., Phys. Rev. Lett. 82, 3568 (1999)

# Ab initio multi-reference perturbation theory calculations of the low-lying states of the YbCs molecule

D.N. Meniailava\*, M.B. Shundalau
Belarusian State University, Nezavisimosti ave. 4, Minsk, Belarus, 220030
\*E-mail: darhon.yo@gmail.com

Nowadays polar diatomic molecules comprising atoms of different alkali metals offer prospects for using such molecules in the development of quantum computers [1], for testing the fundamental theory of the electric dipole moment of the electron, for controlled chemical reactions at extremely low temperatures. In this case it is necessary to know the exact forms of the potential energy curves (PECs) of the electronic states, as well as the spectral, energetic and dynamic characteristics of their rovibronic states. The *ab initio* calculations of the electronic terms allow to compute all of the necessary characteristics of the rovibronic states. The system of electronic states of the molecule YbCs has not been investigated experimentally and therefore *ab initio* calculations are the actual task.

In this study, the SA-CASSCF(3,12)/XMCQDPT2 [2] calculations of the low-lying doublet states ( $X^2\Sigma^+$ ,  $2^2\Sigma^+$ ,  $1^2\Pi$ ) and the spin-orbit coupling (SOC) with the one-electron Pauli-Breit operator for the YbCs molecule are performed (Fig. 13). Such calculations were carried out in work [3] for KRb and YbRb molecules and indicated good agreement with experimental data. Therefore, correct results are expected for YbCs molecule. The Stuttgart RSC ECPs are used in the calculations. At the dissociation limit Yb(6s²) + Cs(6p) the energies of the lowest excited YbCs terms relatively to the its ground state (according to NIST) are 11178.3 and 11732.3 cm $^{-1}$  with the SOC splitting equals 554.0 cm $^{-1}$ . The corresponding calculated energies of the low-lying terms relatively to the ground state at the distance of 17.0 Åare: 11177.8 ( $\Omega=1/2$ ) and 11732.3 cm $^{-1}$  ( $\Omega=3/2$ ) with the SOC splitting equals 554.5 cm $^{-1}$ . These data show that our calculations well agree with experimental energies at the dissociation limit. Potential well depth for the ground state is 158.7 cm $^{-1}$  at the distance of 5.775 Å.

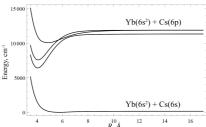


Figure 4: Calculated at the CASSCF(3,12)/XMCQDPT2 + SOC level of theory low-lying terms of the YbCs molecule in the range from 3.5 to 17.0  $\mathring{\text{A}}$ 

- [1] O. Dulieu, C. Gabbanini, Rep. Prog. Phys. **72**, 086401-1-086401-10 (2012)
- [2] A.A. Granovsky, J. Chem. Phys. 134, 214113-1-214113-14 (2011)
- [3] M.B. Shundalau, Private communication

### High-resolution spectroscopy of IRAS22272 + 5435

Laimons Začs<sup>1,2</sup>, Faig A.Musaev<sup>3,4,5</sup>, Bogdan Kaminskyi<sup>6</sup>, Yakiv Pavlenko<sup>6</sup> Aija Grankina<sup>1</sup>, Julius Sperauskas<sup>2</sup>, and Bruce J. Hrivnak<sup>7</sup>

<sup>1</sup>Laser Center, University of Latvia, Rainis blvd. 19, Riga, LV-1586, Latvia
 <sup>2</sup>Vilnius University Observatory, Čiurlionio 29, Vilnius 2009, Lithuania
 <sup>3</sup>Special Astrophysical Observatory of the Russian AS, Nizhnij Arkhyz, 369167, Russia
 <sup>4</sup>Institute of Astronomy of the Russian AS, 48 Pyatnitskaya st., 119017, Moscow, Russia
 <sup>5</sup>Terskol Branch of Institute of Astronomy of the Russian AS, 361605 Peak Terskol, Kabardino-Balkaria. Russia

<sup>6</sup>Main Astronomical Observatory of Academy of Sciences of Ukraine, Zabolotnoho 27, Kyiv, 03680, Ukraine

The proto-planetary nebula (PPN) phase is an important but still poorly understood stage in the evolution of low- and intermediate-mass stars. A PPN is characterized by a central star with effective temperature from 5000 to 30000 K surrounded by an expanding circumstellar envelope of molecular gas and cool dust.

A time series of high-resolution spectra was observed in the optical wavelength region for the proto-planetary nebula IRAS22272 + 5435, along with a simultaneous monitoring of its radial velocity and magnitudes.

The object is known to vary in light, color, and velocity due to pulsation with a period of 132 days.

The light and color variations are accompanied by significant changes in spectral features, most of which are identified as lines of carbon-bearing molecules. According to the observations, the  $C_2$  Swan system and CN Red system lines are stronger near the light minimum. A photospheric spectrum of the central star was calculated using new self-consistent atmospheric models. The observed intensity variations in the  $C_2$  Swan system and CN Red system lines were found to be much larger than expected if due solely to the temperature variation in the atmosphere of the pulsating star. In addition, the molecular lines are blueshifted relative to the photospheric velocity. The site of formation of the strong molecular features appears to be a cool outflow triggered by the pulsation. The variability in atomic lines seems to be mostly due variations of the effective temperature during the pulsation cycle. The profiles of strong atomic lines are split, and some of them are variable in a time scale of a week or so, probably because of shock waves in the outer atmosphere [1].

The European Union FP7-PEOPLE-2010-IRSES program is acknowledged for funding exchange visits in the framework of the project POSTAGBinGALAXIES (grant agreement No. 269193).

#### References

[1] Začs, L., Musaev, Kaminskyi, B., Pavlenko, Y., Grankina, A., Sperauskas, J., and Hrivnak B.J. The Astrophysical Journal **816**, 3 (2016)

<sup>&</sup>lt;sup>7</sup>Department of Physics and Astronomy, Valparaiso University, Valparaiso, IN 46383, USA \*E-mail: aija.laure@gmail.com,

# Analysis and modeling of absorption spectrum for metal-poor star TT CVn

Aija Grankina<sup>1,\*</sup>, Laimons Začs<sup>1,2</sup>, Julius Sperauskas<sup>2</sup>, Viktoras Deveikis<sup>2</sup>, Bogdan Kaminskyi<sup>3</sup>, Yakiv Pavlenko<sup>3</sup> and Faig A.Musaev<sup>4</sup>

<sup>1</sup>Laser Center, University of Latvia, Rainis blvd. 19, Riga, LV-1586, Latvia <sup>2</sup>Vilnius University Observatory, Čiurlionio 29, Vilnius 2009, Lithuania <sup>3</sup>Main Astronomical Observatory of Academy of Sciences of Ukraine, Zabolotnoho 27, Kyiv, 03680, Ukraine

<sup>4</sup>Special Astrophysical Observatory of the Russian AS, Nizhnij Arkhyz, 369167, Russia \*E-mail: aija.laure@gmail.com,

The wide-field spectroscopic surveys revealed a high frequency of carbon-rich stars among old metal-poor stars. The chemical abundances of such stars reflect the origin of CNO and neutron-capture elements in the early Galaxy. Radial velocity measurements and high-resolution spectroscopy in the wavelength region from blue to near infrared are employed in order to clarify the evolutionary status of the carbon-enhanced metal-poor star TT CVn with unique ratio of carbon isotopes in the atmosphere. New high-resolution spectrum was observed with the echelle spectrometer MAESTRO at the Observatory on the Terskol Peak in Northern Caucasus (see Fig. 1). The standard DECH20T routines [2] were used for the spectrum processing.

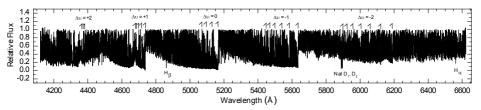


Figure 5: Normalized high resolution spectrum of TT CVn in the wavelength region from 4100 to 6650 Å. The dominating  $C_2$  Swan system  $\Delta v = +2, +1, 0, -1, -2$  bandheads and a few prominent atomic lines are marked.

Radial-velocity monitoring was performed using the CORAVEL spectrometer of the Vilnius University. An abundance analysis was carried out using the method of spectral synthesis and new atmospheric models. The radial velocity monitoring confirmed semiregular variations with a peak-to-peak amplitude of about 10 km  $s^{-1}$  and a dominating period of about 115 days. The iron abundance in the atmosphere of TT CVn was calculated to be about 200 times lower than solar. Carbon to oxygen and carbon isotope ratios are found to be extremely high, C/O  $\approx 12.6$  and  $^{12}C/^{13}C > 1500$ , respectively. TT CVn could be a single old low mass pulsating star.

The European Union FP7-PEOPLE-2010-IRSES program is acknowledged for funding exchange visits in the framework of the project POSTAGBinGALAXIES (grant agreement No. 269193) [1].

- [1] Začs, L., Sperauskas, J., Grankina, A., Deveikis, V., Kaminskyi, B., Pavlenko, Y., Musaev, F.A. The Astrophysical Journal **803**,17 (2015)
- [2] http://www.gazinur.com/Spectra-Processing.html/

## Distributed feedback structure period determination for thin film lasers of DCM derivatives in PVK matrix

Andris Pavils Stikuts\*, Martins Narels, Aivars Vembris
Institute of Solid State Physics, Kengaraga 8, Riga, Latvia, LV-1063
\*E-mail: apstikuts@gmail.com,

DCM is a widely used organic laser dye, however, DCM intermolecular interactions at high concentrations create agregates that negatively influence its optical properties. At Riga Technical University DWK-1, DWK-2, DWK-1TB have been synthesised to counter this effect. Using a distributed feedback (DFB) structure as a laser resonator provides high reflection at a chosen wavelength. Moreover, this wavelength can be varied by changing the period of the structure. Monochromatic light and low lasing treshold are characteristic for a DFB laser.[1]

The objective of this work was to find the parameters needed to create a DFB structure for thin film lasers. The wavelength of the reflected light in a DFB structure is given by

$$m\lambda_{ref} = 2n_{eff}\Lambda,$$

where  $\lambda_{ref}$  is the wavelength of the reflected light,  $\Lambda$  is the period of corrugation of the DFB structure,  $n_{eff}$  is the effective refractive index of the thin film and m is an integer number. The refractive indices of the substrate, the thin film and the coating (air) as well as the thickness of the film need to be known to determine  $n_{eff}$  for a given wavelength.

Using a profilometer thickness was measured for spin-coated thin films consisting of various concentrations of dye (DCM, DWK-1, DWK-2, DWK-1TB) in a PVK matrix on BK7 glass. The thickness ranged from 350nm to 500nm. Utilising the m-line method refractive indices of the thin films were determined at wavelength  $\lambda=632.5nm$ . It was found that the refractive index increased as the concentration of the dye increased. From the absorption spectrum using Kramers-Kronig relations the refractive indices of the thin films were determined as a function of wavelength and adjusted to the right value from the measurement at  $\lambda=632.5nm$ . The effective refractive index of the thin film was determined for the light, whose wavelength coincides with the maximum of the amplified spontaneous emmision spectrum of the thin film. The second order period of a DFB structure  $\Lambda=\frac{\lambda_{ref}}{n_{eff}}$  was determined for each film such that it reflected light of this wavelength.

#### References

[1] S. Forget, S. Chenais, Organic Solid-State Lasers (Springer, 2013)

# Luminescence of europium and dysprosium co-doped oxyfluoride glasses

<u>Janis Sperga</u>\*, Meldra Kemere, Uldis Rogulis, Jurgis Grube *Institute of Solid State Physics, Kengaraga 8, Riga, Latvia, LV-1063* \**E-mail:* janis.sperga16@gmail.com,

The luminescent glasses and glass ceramics have found various applications in many fields such as color display, general lightning, optical communication, laser technology etc. One of the most perspective classes is oxyfluoride glass-ceramics due to their low phonon energy, good chemical, mechanical and optical stability.[1,2,3] Doped with RE ions these materials can be used as an effective white light luminophores. Though many researchers have investigated luminescence of rare-earth ions co-doped glasses and glass-ceramics, to the best of our knowledge, there are no reports on RE co-doped calcium aluminosilicate glass matrix with  $\text{CaF}_2$  as the nucleating agent.

In the present work, we have investigated luminescence of our matrix co-doped with two ions ( $Eu^{3+}$  and  $Dy^{3+}$ ). The luminescence spectra and interaction mechanisms between activator ions have been analyzed.

Transparent oxyfluoride glasses with composition of  $SiO_2$ - $Al_2O_3$ -CaO- $CaF_2$ , co-doped with  $Eu^{3+}$  and  $Dy^{3+}$  (concentration about 1 mol%), have been synthesized. In order to investigate interaction between the activator ions, different concentration ratios of activators  $Dy^{3+}$ ;  $Eu^{3+}$  (1:0,1:1,1:0.5,0:1) were chosen. The photoluminescence spectra and photoluminescence excitation spectra were measured, as well as photoluminescence decay kinetics, using the excitation range 300-480 nm.

In the co-doped samples, the excitation spectra of  $\mathrm{Eu}^{3+}$  show excitation peaks at the characteristic excitation wavelengths of  $\mathrm{Dy}^{3+}$  (350 nm and 453 nm). Luminescence spectra show that emission intensity of  $\mathrm{Dy}^{3+}$  ions in co-doped samples is much lower with respect to  $\mathrm{Dy}^{3+}$  single-doped sample. Furthermore, a changes in luminescence decay curves are also observed. These findings indicate, that an energy transfer from  $\mathrm{Dy}^{3+}$  to  $\mathrm{Eu}^{3+}$  ions occur in the investigated samples.

- [1] P.P.Fedorov, A.A.Luginina, A.I.Popov, Journal of Fluorine Chemistry 172, 22-50 (2015)
- [2] G.Anjaiah, SK.Nayab Rasool, P.Kistaiah, Journal of Luminescence 159, 110-118 (2015)
- [3] V.Nazabal, M.Poulain, M.Olivier, P.Pirasteh, P.Camy, J.L.Doualan, S.Guy, T.Djouama, A.Boutarfaia, Journal of Fluorine Chemistry **134**, 18-23 (2012)

### Spectroscopic study of the bright star HD179821

<u>Mārcis Greiselis</u>\*, Laimons Začs *Laser Centre, University of Latvia, Rainis blvd. 19, Riga, Latvia, LV-1586* \**E-mail*: greiselis@inbox.lv,

The Infrared Astronomical Satellite (IRAS) sky survey has discovered many objects with low colour temperature, some of which may be objects in a transition phase between the asymptotic giant branch (AGB) and planetary nebulae (PN). The identification and research of these transition objects is important in the understanding of the formation mechanism of PN and the enrichement of the circumstellar environment by nuclear processed matter. Detailed spectroscopy of these objects may help us to understand their evolutionary stage and contribute further researches.

HD179821 is a bright star with visual magnitude about 8.3 mag and a very large infrared ekscess at 25 and 60 µm, similar to that observed in PN [1]. The optical spectrum of HD179821 shows that the star is a high-luminosity object and the presence of a detached cool dust shell suggests that it has experienced mass loss in the recent past. The measurements of expansion velocity for the circumstellar shell give about 30 km/s [2], which is larger than the average value for AGB stars. Therefore, this enigmatic object have characteristics of both a pre-planetary nebulae stars and a yellow hyper-giants, so the evolutionary stage has been debated for HD179821 more than 20 years. A new high-resolution spectrum in the optical region was observed with echelle spectrometer TUVES fed by the 2 m telescope at the Observatory on the Terskol Peak near Elbruss at altitude of 3100 meters on 2014 October 7. The spectrum was processed using the standard DECH20T package. Absorption lines are identified, wavelength (Doppler) shifts and equivalent widths are measured, and abundances are calculated using the method of atmospheric models to clarify the evolutionary stage for this extraordinary star.

- [1] Začs L., Klochkova V.G., Panchuk V.E., Spēlmanis R., 1996, Mon. Not. R. Astron. Soc., vol. 282, 1171-1180
- [2] Van der Veen, W.E.C.J., Trams, N.R., Waters, L.B.F.M., 1993, A&A, vol.269, 231

# Modeling of Optically detectable magnetic resonances of nitrogen - vacancy optical centers in diamond crystal

 $\underline{Reinis\ Lazda}^{1,*},$ Mārcis Auziņš $^1$ , Laima Bušaite $^1$ , Linards Kalvāns $^1$ , Jānis Šmits $^1$ , Agris Špīss $^1$ 

<sup>1</sup>Laser Centre, University of Latvia, Rainis blvd. 19, Riga, Latvia, LV-1586 \*E-mail: lazdareinis@gmail.com,

The NV center is a point deffect in a diamond crystal lattice consisting of a carbon atom substituting nitrogen atom (N) and a vacancy (V) pair, see Fig. 13a [1]. The energy level scheme used is shown in Fig. 13b [2].

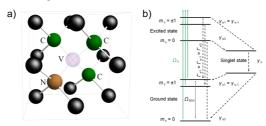


Figure 6: a) Schematic image of a NV center in a diamond lattice, black - carbon atoms, orange - nitrogen atom, white (transparent) - vacancy b) Considered energy level scheme of a NV center, where  $\Gamma$ ,  $\gamma$  - relaxation rates,  $\Omega_R$  - pump laser Rabi frequency,  $\Omega_{MW}$  - scanned microwave Rabi frequency.

The energetic structure of the NV center is described using the spin Hamiltonian method, see equation (1),

$$H = g_e \mu_b \mathbf{B} \mathbf{S} + \mathbf{S} \hat{\mathbf{D}} \mathbf{S} \tag{1}$$

where  $g_e$  - electron Lande factor,  $\mu_B$  - Bohr magneton,  ${\pmb B}$  - external magnetic field vector,  ${\pmb S}$  - operator of the electron spin S=1,  $\hat{{\pmb D}}$  - zero (external magnetic field) splitting tensor [3]. Modeling of Optically detectable magnetic resonances (ODMR) of nitrogen - vacancy (NV) optical centers in diamond crystal is done. Modeled ODMR signals taking into account only the ground state of the NV center are obtained and compared with experimentally obtained data (qualitative agreement of modeled ODMR signals and experimental data can be seen). A model that includes the ground state, excited state and a intermediate singlet state is considered for development. NV centers can be potentially used as quantum registers (for example, in quantum computers) and for magnetic field measuring (magnetometry). NV centers have a discrete (similar to atoms) energy level structure in a solid.

### Acknowledgements

This study was supported by the M-ERA.NET project MyND no. Z/15/1366.

- [1] Lloyd C.L. Hollenberg et al., Physics Reports 528 1, 1-46 (2013)
- [2] Dumeige et al., Phys. Rev. B 87, 155202 (2013)
- [3] A. P. Nizovtsev et al., Opt. Spectrosc. 108 (2), 230-238 (2010)

# Deconvolution - a tool for enhanced resolution magnetic images

Janis Smits<sup>1</sup>, Florian Gahbauer<sup>1</sup>, Andris Berzins<sup>1</sup>, Kaspars Erglis<sup>2</sup>

<sup>1</sup>Laser Centre, University of Latvia, Zellu street 25, Riga, Latvia, LV-1002

<sup>2</sup> MMML Lab, Faculty of Physics and Mathematics, University of Latvia, Riga, LV-1002, Latvia

\*E-mail: smitsjanis@gmail.com,

Nitrogen vacancy (NV) centers in diamond have shown great promise for magnetic field measurements and have recently been used to to image magnetic field distributions in biological systems [1]. However as the scale of observed fields reaches that of optical wavelengths, optical resolution poses a problem for obtaining high quality magnetic images.

In this work the possibility of using deconvolution methods to enhance the resolution of magnetic images was examined. A forward problem was solved assuming ideal dipoles and various distances from NV centers. Two deconvolution algorithms were examined (the Wiener filter and Richardson-Lucy deconvolution), examining their behavior with different noise and blurring kernels applied to the images. Finally the effect of depth density distribution of NV centers is incorporated in the model. The forward problem consists of obtaining the real magnetic field of an ideal dipole, generating Lorentz distributions with an expectation value that matches the magnetic field, blurring the image by discrete convolution and applying Poisson noise.

### Ackowledgements

This study was supported by the M-ERA.NET project MyND no. Z/15/1366.

#### References

[1] D. Le Sage, K. Arai, D. R. Glenn, S. J. DeVience, L. M. Pham, L. Rahn-Lee, M. D. Lukin, A. Yacoby, A. Komeili, and R. L. Walsworth, Nature **496**, 486 (2013).

# Photoluminescence in 2D transition metal dichalcogenide nanostructures

Edgars Butanovs\*, Boris Polyakov, Janis Zideluns, Alexei Kuzmin, Jelena Butikova
Institute of Solid State Physics, Kengaraga 8, Riga, Latvia, LV-1063
\*E-mail: edgarsbutanovs@gmail.com

In recent years transition metal dichalcogenide materials have attracted significant attention due to their unusual properties in the nanoscale. Semiconducting material, such as  $WS_2$  and  $MoS_2$ , two-dimensional nanostructures have direct band gaps, compared to indirect band gap in their bulk counterparts, therefore such nanostructures offer numerous potential applications in optoelectronics, sensing, microelectronics, and due to their layered structure and high specific surface area also in nanotribology, catalysis etc. Strong room-temperature photoluminescence has been previously reported in both  $WS_2$  [1] and  $MoS_2$  [2] atomically thin two-dimensional crystals.

 $WS_2$  and  $MoS_2$  triangular nanostructures were grown on a silica wafer and  $MoS_2$  nanostructures on a sapphire wafer by atmospheric pressure chemical vapour deposition. Optical microscope, scanning electron and atomic force microscope, and Raman spectroscopy was used to characterize grown nanostructures. Photoluminescence with a peak at 677 nm was measured in  $MoS_2$  nanocrystals, and with a peak at 640 nm in  $WS_2$  nanocrystals. Relation between nanocrystal thickness and photoluminescence intensity is discussed.

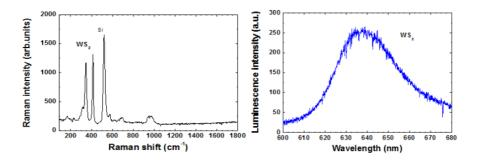


Figure 7: Measured Raman (*left*) and luminescence (*right*) spectrum of a WS<sub>2</sub> nanostructure on a silica wafer.

- [1] Humberto R. Gutierrez et al. Nano Letters **13 (8)**, 3447 3454 (2013)
- [2] Kin Fai Mak, Changgu Lee, James Hone, Jie Shan and Tony F. Heinz. Physical Review Letters **105**, 136805 (2010)

# Structure of Gd<sup>3+</sup> ions in oxyfluoride glass ceramics containing fluorite crystallites

Andris Antuzevics\*, Meldra Kemere, Reinis Ignatans
Institute of Solid State Physics, Kengaraga 8, Riga, Latvia, LV-1063
\*E-mail: andris.antuzevics@gmail.com,

Oxyfluoride glass ceramics doped with rare earth ions are attractive materials as optically active media. [1] It is necessary to study the structure of luminiscence centres in order to improve optical properties of such materials.

Electron paramagnetic resonance (EPR) spectroscopy is a structure sensitive method for point defect study. In this work it is used to detect the surrounding environment of  $Gd^{3+}$  impurities in fluorite structure nanocrystals ( $CaF_2$ ,  $SrF_2$ ,  $BaF_2$ ) embedded in the glass matrix. The EPR measurements of the glass samples show that  $Gd^{3+}$  is located in a disordered environment, however in glass ceramics for each crystallite a characteristic fine structure emerges. The formation of crystallites is controlled with X-ray diffraction (XRD) measurements.

Fine structure parameter analysis indicates that the cubic, tetragonal and trigonal  $\mathrm{Gd}^{3+}$  centres have been observed in the studied glass ceramics. The EPR spectra simulations are presented in this work.

#### References

[1] P.P. Fedorov, A.A. Luginina, A.I. Popov, J. Fluor. Chem. **172**, 22-50 (2015)

# Luminescence and quantum efficiency of europium doped oxyfluoride glasses and glass-ceramics

Meldra Kemere<sup>1,\*</sup>, Uldis Rogulis<sup>1</sup>, Stefan Schweizer<sup>2,3</sup>, Franziska Steudel<sup>3</sup>, Sebastian Loos<sup>2</sup>, A. Charlotte Rimbach<sup>2</sup>, Reinis Ignatans<sup>1</sup>

<sup>1</sup>Institute of Solid State Physics, University of Latvia, 8 Kengaraga Street, 1063 Riga, Latvia <sup>2</sup>Department of Electrical Engineering, South Westphalia University of Applied Sciences, Luebecker Ring 2, 59494 Soest, Germany

<sup>3</sup>Fraunhofer Application Center for Inorganic Phosphors, Branch Lab of Fraunhofer Institute for Microstructure of Materials and Systems IMWS, Luebecker Ring 2, 59494 Soest, Germany \*E-mail: meldra.kemere@gmail.com,

Oxyfluoride glasses and glass-ceramics are considered as promising materials for photonic applications including light emitting diodes due to their good optical properties they combine. Oxide glass matrix is characterized with good stability, whereas fluoride crystallites have low phonon energy.

Within the framework of this research, photoluminescence (PL) spectra and quantum efficiency of Eu-doped  $SiO_2$ - $Al_2O_3$ - $ZnF_2$ - $SrF_2$  (SAZS) and  $SiO_2$ - $Al_2O_3$ -CaO- $CaF_2$  (SACC) oxyfluoride glasses and glass-ceramics have been investigated. The glass samples have been prepared by the melt quenching method in air atmosphere, while the glass-ceramics were obtained by the heat treatment method from the "as-made" samples. Differential scanning calorimetry and X-ray diffraction measurements were performed.

In the PL spectra of the  $Eu^{3+}$  glasses, the electric dipole transitions are dominant, which are characteristic for low symmetry environment of glasses. On the contrary, in the PL spectra of the SAZS  $Eu^{3+}$  -doped glass-ceramics the magnetic dipole transitions are dominant due to the fact that a higher symmetry environment of  $Eu^{3+}$  centres has been identified. The observed quantum efficiency is higher for SACC samples (70%) as compared to the SAZS samples (64%). In the "as-made" SAZS samples, initially only the trivalent  $Eu^{3+}$  luminescence has been observed, whereas, in the glass-ceramics the luminescence of divalent europium  $Eu^{2+}$  has been recorded.

The project of the Baltic-German University Liaison Office was supported by the German Academic Exchange Service (DAAD) with funds from the Foreign Office of the Federal Republic Germany.

### Modelling second-order optical non-linearity of organic material through simple quantum chemical calculations

Igors Mihailovs<sup>1,2,\*</sup>, Kaspars Traskovskis<sup>2</sup>, Martins Rutkis<sup>1</sup>

<sup>1</sup>Institute of Solid State Physics, Kengaraga 8, Riga, Latvia, LV-1063 <sup>2</sup>Institute of Applied Chemistry, Riga Technical University, P. Valdena St. 3, Riga, Latvia, LV-1048

\*E-mail: igorsm@cfi.lu.lv,

In the last decade, there is considerable interest in organic non-linearly-optically (NLO) active chromophore molecules with bulky groups.[1,2] These are incorporated to mitigate chromophore aggregation which lowers second-order NLO activity of the material. Bulky groups usually have no prominent effect on electronic properties of matter because of no conjugation with the easily-polarizable electronic system. Moreover, when thermalized, these groups are easily changing their orientation with respect to the chromophore, causing random fluctuations in the dipole moment, which is also important characteristic of a NLO-active molecule. This fluctuating part is loosely relevant to orientation of chromophores in external electric field, which is the usual way to produce non-centrosymmetric organic NLO materials.[1,2] Thus, it was of interest to compare how is the calculation affected by exclusion of bulky groups from the structure; and experiment data are found to be approximated better by truncated structures than by full ones.

In addition, we compared performance of various calculation methods. Within CPHF or CPKS approach HF method is known to produce rather qualitative polarizabilities,[3] although it can be inferior to DFT methods.[4] Particularly, range-separated hybrid functionals (RSH) are promoted for calculating hyperpolarizability.[3,5] However, bondlength alternation (BLA) is sometimes reported to be predicted best by classical hybrids,[6] while other studies support usage of RSH.[7] Calculated NLO properties are known to depend strongly on BLA.[3,8] Solvent and frequency dependence of results, contrarily, can often be neglected.[4] In our study, we considered four 2-(4-aminobenzylidene)-1,3-indandione analogues and found out that RSH CAM-B3LYP outperforms both HF and B3LYP in calculating the product of dipole moment and first hyperpolarizability  $\mu\beta_0$  as an estimate for macroscopic non-linearity index  $d_{33}$ . However, BLA is better modelled by B3LYP, while HF fails dramatically in reproducing it.

- [1] Z. Li, G. Qiu, Ch. Ye, et al., Dyes Pigm. **94**, 16-22 (2012)
- [2] M. D. H. Bhuiyan, M. Ashraf, A. Teshome, et al. Dyes Pigm. 89, 177-187 (2011)
- [31] S.-I Lu, Chem. Phys. Lett. **581**, 42-46 (2013)
- [4] K. Yu. Suponitsky, S. Tafur, A. E. Masunov, J. Chem. Phys. 129, 044109 (2008)
- [5] S.-I Lu, J Comput Chem **32**, 730-736 (2011)
- [6] D. Jacquemin, E. A. Perpète, I. Ciofini, C. Adamo, Chem. Phys. Lett. **405**, 376-381 (2005)
- [7] P. A. Limacher, K. V. Mikkelsen, H. P. Lüthi, J. Chem. Phys. **130**, 194114 (2009)
- [8] C. B. Gorman, S. R. Marder, Proc. Natl. Acad. Sci. USA 90, 11297-11301 (1993)

### $Pr^{3+}$ luminescence in oxyfluriode glass and oxyfluoride glass ceramic containing NaLaF $_4$

Girts Zageris, Jurgis Grube, Anatolijs Sarakovskis, Guna Krieke *Institute of Solid State Physics, Kengaraga 8, Riga, Latvia, LV-1063*\*\*E-mail: girts.zageris@fizmati.lv,

Rare-earth activated oxyfluoride glass and glass ceramics are interesting luminescent materials - their chemical compositions are identical, but luminescence properties are different. The mechanisms that govern how rare-earth ions incorporate into the crystallographic lattice and, subsequently, processes of luminescence are different for glass and glass ceramic materials. These mechanisms are what this research focuses on.

Oxyfluoride glass samples with various concentrations (0.01, 0.1 and 1 mol%) of praseodymium were obtained, with each of these samples having been synthesized under similar circumstances. Afterwards, the glass samples were heated once more in different temperatures in order to obtain glass ceramic samples containing NaLaF<sub>4</sub> crystalline phase. Luminescence spectra both for glass and glass ceramic samples were measured at room temperature as well as low (10 K) temperature. Luminescence kinetics of various luminescence bands were also obtained. The accumulated data allows to conclude that the mechanisms behind luminescence in glass and glass ceramic are indeed different, and they are dependent on the concentration of the rare-earth ion in a given sample. Based on experimental results, the impact on luminescence of the concentration of praseodymium in glass and glass ceramics is discussed.

#### Cloud Monte Carlo for the needs of biomedical optics

Igor Meglinski<sup>1</sup>

<sup>1</sup> Department of Physics, University of Otago, New Zealand \*E-mail: igor@physics.otago.ac.nz,

Conceptual engineering design and optimization of laser-based imaging techniques and optical diagnostic systems used in the field of biomedical optics requires a clear understanding of the light-tissue interaction and peculiarities of localization of the detected optical radiation within the medium. The description of photon migration within the turbid tissue-like media is based on the concept of radiative transfer that forms a basis of Monte Carlo (MC) modelling. An opportunity of direct simulation of influence of structural variations of biological tissues on the probing light makes Monte Carlo a primary tool for biomedical optics and optical engineering. Due to the diversity of optical modalities utilizing different properties of light and mechanisms of light-tissue interactions a new Monte Carlo code is typically required to be developed for the particular diagnostic application. By introducing an object oriented concept of Monte Carlo modelling and utilizing modern web applications we present the generalized and unified computational tool suitable for the major applications in Biophotonics and Biomedical Optics.

### Modeling skin diffuse reflectance spectra in the near-infrared and visible spectral range

Gatis Tunens, Inga Saknite, Janis Spigulis

Biophotonics Laboratory, Institute of Atomic Physics and Spectroscopy, Raina Blvd 19, Riga, LV-1586, Latvia

Monte Carlo method was used in this research to simulate diffuse reflectance spectra of human skin. This method allows non-invasive diagnosis of the human skin by measuring diffuse reflectance spectra of the skin and comparing the spectra to results simulated by a computer model (see Fig. 8). If the spectra match, optical parameters of the model

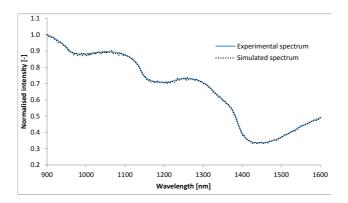


Figure 8: Experimentally taken diffuse reflectance spectra compared to the simulated diffuse reflectance spectra in the near-infrared spectral range.

can be attributed to the skin that the experimental spectra was measured from. Based on the Monte Carlo simulation program created by *Wang and Jacques* (1995)[1], a *Matlab* based graphical user interface was created with the ability to input various parameters (absorption coefficient, layer structure, refractive indices, spectral range and resolution) and simulate a diffuse reflectance spectrum, or input an experimental spectrum and automatically simulate the optical parameters of the model inversely. Various coefficient changes were tested to learn their effect on the simulated spectra. The simulation source code was modified to gather 3D output data about source-detector separation. The result of this research shows potential in determining the optical properties of human skin by a non-invasive, inverse Monte Carlo approach.

#### References

[1] Wang, L-H, S.L. Jacques, L-Q Zheng: MCML - Monte Carlo modeling of photon transport in multi-layered tissues. Computer Methods and Programs in Biomedicine 47:131-146, 1995.

#### Acknowledgements

This work was supported by Latvian National research program SOPHIS under grant agreement Nr.10-4/VPP-4/11

#### Selective Plane Illumination Microscope Using Non-Spreading Airy Beams

A. Leitis<sup>1,\*</sup>, J. Axelsson<sup>1</sup>

<sup>1</sup> Department of Physics, Lund University, P.O. Box 118, 22100 Lund, Sweden \*E-mail: leitis.aleksandrs@gmail.com,

Recently a new field of microscopy has emerged, known as selective plane illumination microscopy (SPIM). Using SPIM setup the sample is illuminated with a thin light sheet from the side. The selective plane illumination overcomes many problems that conventional microscopes have. Conventional microscopes illuminate the sample axially and collects the light only from the focal plane of the microscope objective. Therefore parts of the sample which are out of focus are illuminated unnecessarily, leading to rapid fluorophore photobleaching and decrease of signal to noise ratio due to out of focus light. The SPIM method overcomes these problems, because only the fluorophores in the focal plane of the objective are excited. Another problem with conventional microscopes is that they are capable only of 2 dimensional imaging. The exception are confocal microscopes, but these microscopes are slow and the field of view is restricted to few hundred micrometers. The SPIM method significantly improves the 3 dimensional imaging speed and can reach up to few hundred frames per second. This imaging speed enhancement is achieved, because the whole plane is captured with a single snapshot, instead of point by point scanning as it happens in confocal microscopes.

To take all the advantages of the SPIM method it is crucial to form a thin light sheet that extends for the whole field of view. Commercially available lasers have Gaussian beam profile. It is well known that tightly focused Gaussian beams spread out quickly, therefore there will be good axial resolution only in the central part of the image. Because of that the field of view will be restricted to the Rayleigh range of the Gaussian beam. In this work we present how to create non-spreading Airy beams using only two additional lens elements and how they can be implemented in the SPIM setup to significantly extend the field of view keeping high axial resolution. This is an important advancement since Airy beams would allow larger sized objects, e.g. optically cleared tissue specimens, to be imaged with high resolution.

### Diffuse Reflectance Spectroscopy for evaluation of tissue chromophore composition

<u>Lisa Kobayashi Frisk<sup>1,\*</sup></u>, Stefan Andersson Engels<sup>1</sup>, Johan Axelsson<sup>1</sup>

Department of Physics, Lund University, P.O. Box 118, 22100 Lund, Sweden

\*E-mail: lisa@frisk650.org

Diffuse Reflectance Spectroscopy (DRS) is a technique where light is sent onto biological tissue using optical fibers. The diffusely remitted photons are collected, some distance from the source, after passing through the tissue. In order to perform quantitative analysis of the DRS spectra, the inverse problem needs to be solved where a theoretical model of the photon migration is fitted to the measured spectrum. In this work a DRS instrument consisting of a fiber optic probe connected to a broadband light source and two spectrometers was developed. In this way, live reference measurements are taken allowing spectra to be measured and calibrated online independent of fluctuations in lamp intensity.

In order to evaluate the calibrated spectra, an evaluation protocol was implemented to determine the absorbing chromophores and scattering parameters of the probed medium. The evaluation protocol was based either on the Diffusion Equation or Monte Carlo lookup tables. The two models and their respective evaluation protocols are also compared with each other based on measurements in liquid optical phantoms made from varying concentrations of whole blood, intralipid and water. In addition the oxygen saturation was varied in the optical phantoms. This work aims to determine the accuracy of evaluating the composition of these phantoms using the evaluation protocols based on either the Diffusion Equation or a Monte Carlo method. The instrument being developed in this project will ultimately be used to track oxygenation and blood volume changes in tumours during radionuclide therapy.

### Mapping of skin chromophores by snapshot taken with a smartphone

Ilze Oshina\*, Zigmars Rupenheits, Janis Spigulis
Biophotonics Laboratory, Institute of Atomic Physics and Spectroscopy, University of Latvia,
Rainis blvd. 19, Riga, LV-1586, Latvia
\*E-mail: osina.ilze@gmail.com,

Skin chromophore maps provide useful information about skin health status. We propose a way of mapping three chromophores - melanin, oxy-hemoglobin and deoxy-hemoglobin - by using a trichromatic illumination and a smartphone.

For illumination we used specially created prototype with three laser module pairs emitting at 448 nm, 532 nm and 659 nm wave length. The smartphone was fixed on the surface of the prototype. Almost all automatic camera settings were switched off. The images were processed on computer using MATLAB software. Trichromatic images were converted into three monochromatic images by separate registration of the R, G and B output values from each image pixel [1]. For chromophor mapping we used an algorithm as described previously [2].

Images obtained from white paper showed uniform illumination confirming suitability for mapping of skin chromophores. Further, the prototype was used in clinical tests to obtain images of vascular and pigmented skin lesions. Results showed increased oxyhemoglobin level and decreased deoxyhemoglobin level in vascular pathologies, and increased melanin level in pigmented lesions compared to the adjacent healthy skin.

To conclude, this prototype has a potential as a simple and inexpensive device for several clinical applications.

This work was supported by the Latvian national research program SOPHIS under the grant agreement #10-4/VPP-4/11.

- [1] J. Spigulis, L. Elste. Single-snapshot RGB multispectral imaging at fixed wavelengths: proof of concept. Proc.SPIE, 8937, 89370L (2014).
- [2] J. Spigulis, I. Oshina. Snapshot RGB mapping of skin melanin and hemoglobin. J.Biomed. Opt., **20(5)**, 050503 (2015).

#### The compound mechanism of adaptation to high contrast

Olga Danilenko<sup>1</sup>, Maris Ozolinsh<sup>1,2</sup>, Varis Karitans<sup>2</sup>, Varvara Zavjalova<sup>1</sup>

<sup>1</sup>Department of Optometry and Vision Science, University of Latvia, LV 1063 Riga, Latvia

<sup>2</sup>Institute of Solid State Physics, University of Latvia, LV 1063 Riga, Latvia

\*E-mail: odanilenko@inbox.lv,

Adaptation to high contrast stimuli results in set of two separate mechanisms that contribute to temporary loss in contrast sensitivity. The first mechanism is negative afterimage formatting on the retina level, while the second mechanism would be a contrast adaptation occurring in higher level of perception [1, 2]. Summary effect of such adaptation is depended on total time of exposure, the contrast of adaptive stimuli and external factors. A time course of such process was designed via phychophysical experiment. The build up of summary adaptation effect is successfully fitted by exponential approximation. The relaxation to basic level that ensues after the adaptation period is stopped is described by exponential decrease function with time constant equal 3.7 sec. The effect of external factors on summary adaptation is studied and separation of two underlying mechanisms is achieved by various methods. Similar adaptation process is studied with involvement of colour perception.

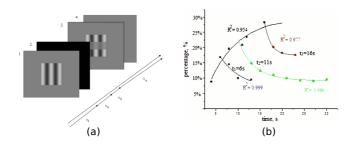


Figure 9: (a) experimental setup; (b) the time course of adaptation.

- [1] A. Kohn, Journal of Neurophysiology **97(5)**, 3155-3164 (2007)
- [2] M.Bao et al, Journal of Vision **13(10)**, 1-11 (2013)

### The impact of position of corneal apex in keratoconus on visual acuity and contrast sensitivity

Sanita Liduma<sup>1\*</sup>, Gunta Krumina<sup>1</sup>,

<sup>1</sup>University of Latvia, Department of Optometry and Vision Science, Riga, Latvia

\*E-mail: sanita.liduma@gmail.com

#### Introduction

Keratoconus is a disease affecting young patients which have to cope with it for the entire life. Patients with keratoconus have changes in the optical quality of the eye and reduced corneal image quality. Patients with keratoconus more sensitive feel that the quality of life worsens in case of changes in the corneal radius of the curvature (> 52 D) and visual acuity with high contrast (<20/40). Patient satisfaction with the quality of life is determined by the following factors: gender of the patient (men are more satisfied), size of the cylinder (at least 1 D) and contrast sensitivity (3 and 6 cpd). Prior to observing decreased acuity of the high contrast sensitivity in patients with keratoconus, changes are observed in contrast sensitivity at medium and high frequencies. Various studies have demonstrated that patients with keratoconus have significant loss of contrast sensitivity, while its value varies in different studies. None of these studies has, however, analysed reduced contrast sensitivity depending on the position of corneal apex, which might explain the various results of the studies. The aim of our study is to assess the correlation between the position of keratoconus corneal apex and the visual acuity and contrast sensitivity. The following hypothesis has been put forward in the study: the closer apex to the central visual axis, the worse the visual acuity and contrast sensitivity data. In order to reach the goal, the following task have been identified: (1) to assess the mutual correlation between the best corrected visual acuity and contrast sensitivity at each stage of keratoconus; (2) to assess how the visual acuity and contrast sensitivity change depending on the position of keratoconus corneal apex; (3) to assess the patient life quality depending on the stage of keratoconus and position of corneal apex.

#### Method

The visual acuity and contrast sensitivity have been evaluated in the study using the FrACT test (developed by M.Bach). The contrast sensitivity has been assessed at the following frequencies: 1, 3, 5, 7, 9, 11, 13 and 15 cpd. So far 8 eyes with keratoconus have been analysed.

#### Results

The first results confirm the hypothesis, i.e. the closer the keratoconus apex to the central visual axis, the poorer the visual acuity and contrast sensitivity. If the keratoconus apex is located in the centre of the cornea, contrast sensitivity is poorer at the medium and high frequencies, while if the apex is located in the peripheral cornea, the loss of contrast sensitivity is only observed at the high frequencies.

#### Conclusion

The obtained results explain the various data from the previous studies, as none of the researchers has analysed the change of contrast sensitivity depending on the location of the keratoconus. The position of corneal apex significantly changes retinal image quality. The closer the apex to the central visual axis, the more corneal optics change creating distorted image on the retina which impairs visual acuity and contrast sensitivity in patients with keratoconus.

### Biological motion processing in central and peripheral visual field

 $\underline{\text{Ilze Laicane}}^{1,*},$  Jurgis Skilters², Vsevolod Liakhovetckii³, Elina Zimasa¹, Gunta Krumina¹

\*E-mail: ilze.laicane@lu.lv,

The question whether the perception of biological motion is equally effective in both central and peripheral visual field is not entirely clear. By using a slightly different experimental setup Ikeda et al. (2005) and Gurnsey et al. (2010) came to completely opposite conclusions.

Here we rise the question on the processes affecting the differences of perception of biological motion in central and peripheral visual field. It is well established that the perception of biological motion includes motion perception, perceptual grouping (by similarity, possibly also by common fate, etc.). It is also possible that the perception of biological motion is similar to analyzing the stimuli of enforced disintegration (first described by White and Milne (1999)).

Current study explores the possible mechanisms that determine the perception of biological motion in central and peripheral visual field. Five experiments were created in order to evaluate and compare the perception of (a) biological motion; (b) simple translational motion; (c) enforced disintegration; (d) perceptual grouping by proximity and (e) perceptual grouping by common fate in central and peripheral visual field. All stimuli were embedded in masking noise and the threshold for perception was calculated as the number of dots sufficient for stimulus recognition. Stimuli were demonstrated in three different eccentricities (0, 15 and 30 degrees) and stimulus magnification was used in order to compensate for reduced visual acuity in peripheral visual field.

Preliminary results demonstrate that when analyzing the number of dots sufficient for biological motion detection all of the participants were able to reach the same threshold level in 4 degrees eccentricity as in central visual field. However in further eccentricities (8 and 15 degrees) the performance slightly deteriorated and only 62 percent of the participants were able to reach the same threshold level.

- [1] Gurnsey, R., Roddy, G., Troje, N.F. Journal of Vision **10(2)**, 1-17 (2010)
- [2] Ikeda H., Blake R., Watanabe K. Vision Research, 45, 1935-1943 (2005)
- [3] Laicane, I., Skilters, J., Lyakhovetskii, V., Zimasa, E., Krumina, G. Perception, **44(SI)**, 237 (2015)

<sup>&</sup>lt;sup>1</sup>University of Latvia, Department of Optometry and Vision Science, Rainis blvd. 19, Riga, Latvia, LV-1586

<sup>&</sup>lt;sup>2</sup>University of Latvia, Center for the Cognitive Sciences and Semantics, Rainis blvd. 19, Riga, Latvia, LV-1586

<sup>&</sup>lt;sup>3</sup>Pavlov Institute of Physiology, Russian Academy of Sciences, St.Petersburg, Russian Federation

### Super resolved and extended depth of focus concepts for remote and ophthalmic imaging systems

Zeev Zalevsky

Faculty of Engineering and the Nanotechnology Center, Bar-Ilan University, Ramat-Gan 52900, Israel

E-mail: Zeev.Zalevsky@biu.ac.il

Digital imaging systems as well as human vision system have limited capability for separation of spatial features. Therefore, the imaging resolution is limited. The reasons to this limitation are related to the effect of diffraction i.e. the finite dimensions of the imaging optics, the geometry of the sensing array and its sensitivity as well as the axial position of the object itself which may be out of focus. In this talk we will present novel photonic approaches and means to exceed the above mentioned limitations and eventually to allow having super resolved imaging systems.

Then, novel all optical extended depth of focus concept based on "interference" effect will be demonstrated for ophthalmic usage and implemented on conventional refractive devices, such as spectacles, contact lenses and intraocular lenses. This extended depth of focus technology is capable of simultaneously correcting various refractive errors, such as myopia, hyperopia, presbyopia, regular/irregular astigmatism, as well as their combinations.

In the last part of the talk a special device mounted on spectacles that allows translation of visual information into spatial tactile stimulation of the cornea, will be discussed. This device can lead blind people to "see" by providing a novel and a non-invasive sensory substitution allowing blind people to perceive images after teaching them to associate the tactile spatial feeling of the stimulation of their cornea to real spatial shapes and images.

#### Manually tunable lens based eye model

Varis Karitans<sup>1,2\*</sup>, Jolanta Logina<sup>2</sup>, Gunta Krumina<sup>2</sup>

<sup>1</sup>Institute of Solid State Physics, Kengaraga 8, Riga, Latvia, LV-1063

<sup>2</sup>Department of Optometry and Vision Science, University of Latvia, Jelgavas 1, Riga, Latvia, LV-1004

\*E-mail: variskaritans@gmail.com,

There are various kinds of mathematical model eyes described in details in [1]. Optical and geometrical parameters vary slightly among these models. Unfortunately, there are only very few real model eyes. We report on the optical and geometrical properties of a new model eye based on a manually tunable polymer lens ML-20-35-NIR-HR.

In Fig. 13 the structure of the model eve is shown schematically.

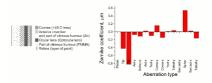


Figure 10: Structure of the model eye.

Using the translation and refraction matrix calculations position of the cardinal (principal, nodal and focal) planes were found. The primary principal plane  $H_1$  is located about 0.9 mm behind the cornea while the secondary principal plane  $H_2$  is located about 3 mm in front of the cornea. The distance between the principal planes and the corresponding nodal planes HN is about 9 mm. The primary focal length  $f_1 = -18.6$  mm, the secondary focal length  $f_2 = 27.5$  mm.

Regarding Zernike aberrations increased levels of both coma-x and coma-y can be observed. This may be due to the liquid polymer lens the shape of which has distorted slightly resulting in coma aberrations. As expected, the spherical aberration has the largest magnitude from all types of higher-order aberrations.

A big advantage of the new model eye is that the adjustable element is the ocular lens like in a living eye. This new model eye has demonstrated potential for being used in ocular accommodation studies and retinoscopy training. If a gel like substance is used to simulate the vitreous humour it would also be possible to simulate vitreous floaters and to study the impact of refractive error on their appearance. However, there are shortcomings characteristic to the optical system of this model eye. Although the equivalent optical power and power tuning range of the model eye is comparable to the corresponding values of a living eye there are strong back-reflections because of deviations of the refractive indices and curvature of surfaces away from the real values. These differences could be minimized by choosing optical media simulating liquids with refractive indices very close to those in a living eye.

- [1] Author, Journal **Volume**, page numbers (year)
- [2] Author, Book title (Publisher, place year)
- [3] http://www.optotune.com/

#### Seasonal environmental spectrophotometry

Sergejs Fomins<sup>1,\*</sup> Janis Kleperis<sup>1</sup>, Maris Ozolinsh<sup>1</sup>

<sup>1</sup>Institute of Solid State Physics, Kengaraga 8, Riga, Latvia, LV-1063

\*E-mail: sergejs.fomins@lu.lv,

The circadian rhythm is controlled by the light and blue light sensitive non-object forming visual system. Light properties impact human health promoting events as day-night cycle, mood, and perception [1]. Latvian geographic location at latitude of 57 degrees north introduces substantial seasonal changes in both, illumination and environmental colorimetry. It is logically to propose that natural colorimetric gamut is shaped by the seasonal conditions. Unfortunately, illuminance or irradiance monitoring stations do not provide the circadian light properties. The annual irradiance data from the solar plantation at Institute of Solid State Physics, University of Latvia, is given in Fig.1.

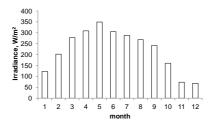


Figure 11: Monthly average irradiance values acquired at UL Institute of Solis State Physics solar plantation. Almost five times differences at winter and summer months.

Our proposed methodology is based on the integral spectral measurements of the illumination information and hyperspectral acquisition of the environmental scenes. We use calibrated Ocean Optics spectrometer equipped with integrating sphere to continuously acquire the spectral information along the calendar year starting from the 2016th. The fragmentary results of the previous spectral data show substantial changes of the photometric quantities of environmental light with less expressed changes of the circadian light. Multispectral analysis of the scenes acquired in previous years showed the reduction of the gamut at red and green components of visual spectrum, while preserving the blue component of the scenes at winter time. However, at least one full annual cycle of circadian light data could provide the important new details relative to human physiology.

#### References

[1] Lucas et al., Trends in Neuroscience **37(1)**, 1-9 (2014)

#### Investigation of photon time-of-flight in human skin

Antra Dzerve<sup>1</sup>, Inesa Ferulova<sup>1</sup>, Alexey Lihachev<sup>1</sup> and Janis Spigulis<sup>1</sup>

<sup>1</sup>Institute of Atomic Physics and Spectroscopy, University of Latvia, Rainis blvd. 19, Riga,

Latvia, LV-1586

\*E-mail: antra\_dzerve@inbox.lv,

The time of flight for photons in human skin was measured using picosecond diode laser. IRF (Instrument Response Function) was compared to a signal that entered and exited the skin. Two different wavelength lasers were used. Time of flight was measured for healthy human skin and a nevus. A difference for time of flight in normal skin and in nevus was observed as well as a difference for different wavelength laser irradiation was observed which allows to conclude that the time photon travels in skin might depend on the characteristics of the medium [1] and wavelength of the irradiation. This can be related to known data for light penetration depth in human skin for different wavelengths. [2]

- [1] R. Rox Anderson, B.S Parrish, M.D., "The Optics of Human Skin", The Journal of Investigative Dermatology, Vol. 77, 13-19 (1981)
- [2] Kamran F, Abildgaard OH, Subash AA, Andersen PE, Andersson-Engels S, Khoptyar D., "Computationally effective solution of the inverse problem in time-of-flight spectroscopy", Optics Express, Vol. 23, 6937 (2015)

### Infrared spectroscopy and imaging for estimation of skin hydration

Reinis Janovskis, Inga Saknite, Janis Spigulis

Biophotonics Laboratory, Institute of Atomic Physics and Spectroscopy, Raina Blvd 19, Riga, LV-1586, Latvia

\*E-mail: reinis.janovskis@hotmail.com,

The goal of this study was to develop a method for estimation of skin hydration in the near-infrared spectral range (900-2500 nm) by using reflectance spectroscopy, as well as to develop a method for mapping of skin hydration in the near-infrared spectral range (900-1700 nm) by using imaging tools. In the near-infrared spectral range, there is high water absorption and also some absorption by lipids in skin [1].

Experimental setup consists of near-infrared spectrometer (Hach DR/2400 portable spectrophotometer) in the spectral range of 900-2500 nm, Y-type water free (WF) optical fiber probe, a halogen bulb light source, and a 3D printed nozzle as a spacer to separate skin from the detection and illumination fibers.

This work has been supported by Latvian National Research Program SOPHIS under the grant agreement 10-4/VPP-4/11 and by Institute for Environmental Solutions.

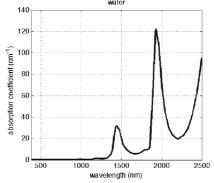


Figure 12: The absorption coefficient of water in  $cm^{-1}$  (380-2500nm), with a resolution of 5 nm [2]

- [1] R. H. Wilson, K. P. Nadeau, F. B. Jaworski, B. J. Tromberg, and A. J. Durkin, "Review of short-wave infrared spectroscopy and imaging methods for biological tissue characterization," J. Biomed. Opt., vol. 20, no. 3, p. 030901, 2015.
- [2] The absorption coefficient of water in [cm-1] (380-2500nm), with a resolution of 5 nm, Natural Phenomena Simulation Group, University of Waterlo, 23.02.2016., http://www.npsg.uwaterloo.ca/data/skin.php

### Figure recognition time in mental rotation task according to their size

Liene Zarina<sup>1</sup>, Jurgis Skilters<sup>2</sup>, Vsevolod Liakhovetckii<sup>3</sup>, Gunta Krumina<sup>1</sup>

<sup>1</sup>University of Latvia, Department of Optometry and Vision Science, Riga, Latvia

<sup>2</sup>University of Latvia, Center for the Cognitive Sciences and Semantics, Riga, Latvia

<sup>3</sup>Pavlov Institute of Physiology, Russian Academy of Sciences, St.Petersburg, Russia

\*E-mail: ziene.larina@gmail.com,

#### Introduction

Several previous studies have confirmed that performance of mental rotation task depends on various factors including sex, age, rotation strategy, and experience in spatial tasks. A factor that has not been explored in details before is the object size. The aim of this study is to determine whether there is a significant impact of figure size on the recognition time in mental rotation task. In addition, we wanted to compare whether there are theoretical links between the results of our study and reading task with different font sizes.

#### Method

A computerized mental rotation task is used. The task contains a pair of 2D or 3D figures where a subject had to judge whether both figures are the same (but rotated) or the second figure is a mirror image of the same figure. Reaction times were measured in all variations. Experimental pairs varied in angular size – 8, 4, 2, and 1 degrees; in total 480 pairs of figures were demonstrated to each subject. 32 subjects participated in our study.

#### Results

Reaction time increase with the increase of rotation angle – this is the main result that has been confirmed in this and most of the previous studies. In general our data indicate that figure size has no impact on the performance of mental rotation test. However, we have that only the smallest of 2D figures does not apply the fact that rotation angle has an impact on test performance. In case of 3D figures all sizes show significant difference between the rotation angle.  $8^{\circ}$  figures in both 2D and 3D objects have a significantly lower number of incorrect answers than in other figure sizes. There was no significant difference in number of mistakes between other sizes.

#### Conclusion

An crucial observation related to our study: a person reads faster and has a better understanding of a text if the letter size is smaller [1]. The following principle seems to be efficient: the larger is the object, the larger are the programmed saccade amplitudes and the more saccades are involved. When a sufficiently small object is observed, the corresponding image is formed straight on the fovea; then it is viewed and rotated directly, the search task is in that case minimal and reaction is fast. That is the reason why we assume that there is no connection between the smallest of 2D figures and the rotation angle at this point.

#### References

[1] Katzir, T., Hershko, S., Halamish, V. (2013). The effect of font size on reading comprehension on second and fifth grade children: bigger is not always better. *Plos One*, 8(9), pp.1-8.

#### Gender differences in mental rotation test

Sabine Matulevica<sup>1\*</sup>, Jurgis Skilters<sup>2</sup>, Vsevolod Liakhovetckii<sup>3</sup>, Gunta Krumina<sup>1</sup> University of Latvia, Department of Optometry and Vision Science, Riga, Latvia <sup>2</sup> University of Latvia, Center for the Cognitive Sciences and Semantics, Riga, Latvia <sup>3</sup> Pavlov Institute of Physiology, Russian Academy of Sciences, St. Petersburg, Russia \*E-mail: sabinematulevica@gmail.com

#### Introduction

Mental rotation is a cognitive process of imagining, mentally rotating and adjusting two and three-dimensional objects. The concept of mental rotation of three-dimensional objects was first introduced by *Shepard and Metzler* in 1971 [1]. In their experiments they found that the reaction time for determining the shape of an object is a relatively linear function of the angular difference between two given three-dimensional objects. It means that if the angle of rotation increases, the reaction time increases as well. Empirical studies on mental rotation show somewhat contradictory results which motivate our study to evaluate differences in time and accuracy between male and female participants. We would also like to explore the gender differences in evaluating 2D and 3D mirrored objects.

#### Method

29 women and 26 men (age 18-30 years) participated in our study. A digitized version of mental rotation test was used. 120 object pairs (60 two- and 60 three-dimensional) were used. Once a pair of objects appears on the computer screen, the subject has to decide whether the objects are the same (but rotated) mirror image of one another. The answer is provided by pressing the corresponding buttons on the computer keyboard.

#### Results

After analyzing the data that we obtained so far, we support *Shepard and Metzler* (1971) assumption that the reaction time is almost a linear function of the angular difference; in other words, if the angular difference increases, the reaction time increases as well. Despite other mental rotation studies, where male participants usually perform better, our first results show no statistical differences between male and female results. Mean reaction time for women, evaluating real 2D and 3D objects, are 2.8 s and 4.6 s, for men 2.7 s and 4.5 s. Mean reaction time in rotating 3D objects is longer than for 2D objects and it is also longer for mirrored objects in both cases.

#### Conclusion

There is no statistical difference between the results of male and female participants and that is contrary to the other authors' studies. The highest error rate occurs with real 3D objects.

#### References

[1] Shepard, R., Metzler, J.,J. Mental rotation of three-dimensional objects, *Science* 171(3972), p.701-703 (1971).

#### Handedness differences in mental rotation task

Annija Gulbe<sup>1\*</sup>, Jurgis Skilters<sup>2</sup>, Vsevolod Liakhovetckii<sup>3</sup>, Gunta Krumina<sup>1</sup>

<sup>1</sup>University of Latvia, Department of Optometry and Vision Science, Riga, Latvia <sup>2</sup>University of Latvia, Center for the Cognitive Sciences and Semantics, Riga, Latvia <sup>3</sup>Pavlov Institute of Physiology, Russian Academy of Sciences, St.Petersburg, Russia \*E-mail: annija.gulbe@gmail.com,

#### Introduction

Mental rotation is a visuo-spatial process enabling mental adjustment objects in a two-dimensional or three-dimensional space. In their research *Shepard and Metzler* (1971) [1] found a linear correlation between increasing rotation angle and response time. Most experiments include pressing with the right hand response button when both objects are recognized as the same (but rotated) and reacting with pressing the left hand button once objects are recognized as different. The main goal of our study is to examine whether the handedness impacts response time and whether it should be considered as a significant factor in future research. The main tasks are as follows: 1) to estimate the possible response time difference in respect to which hand was used to give answer; 2) to assess the possible difference between right-handers' and left-handers' response times; 3) to evaluate the amount of errors made in 2D and 3D stimulus recognition.

#### Method

A special digitalized test was constructed consisting of 120 object pairs (60 two- and 60 three-dimensional). The participant has to indicate whether the objects are similar (but rotated) or reversed (presented as in mirror image). Half of the participants will give confirmative answer using their right hand (group R), other half – using their left hand (group L). At this stage of research total amount of participants are 40 (all right handers), 31 female and 9 males. 18 of them gave answers "same" using their left hand, 22 using right hand.

#### Results

The data shows linearity in growing response time with increased figure rotation angle in both 2D and 3D task. Mean reaction time for group R in 2D was 2.8 s and in 3D 5.1 s; for group L-3.1 s and 5.4 s. Group R responded quicker to mirror images (answer "different" with left hand) in both 2D and 3D task, making more mistakes in 2D task (6,4% errors in the "different" and 3,7% in the "same" tasks).

#### Conclusion

Our results support the linearity initially noticed by Shepard and Metzler(1971) between rotation angle and response time. Regardless of the hand, in both groups 2D objects were rotated faster than 3D. Group R answered the "different" objects (with the left hand) faster but with more errors in 2D task than they answered the "same" objects. The next step of research is to collect a second round of data from the same participants and gather data from left handers as well.

#### References

[1] Shepard, R., Metzler, J.,J. (1971). Mental rotation of three-dimensional objects, *Science* 171(3972), p.701-703.

### Color vision resolution assessment for sorting and forced choice methods

Renars Truksa, Kaiva Jurasevska, <u>Lelde Zabere</u>\* *University of Latvia, Department of Optometry and Vision Science, Riga, Latvia*\*E-mail: lelde.zabere@gmail.com,

For color vision resolution assessment, we used sorting and forced choice methods. Previously known color tests describing these methods are "Farnsworth D-15" test for grouping method and "City University Test" for forced choice method. As we researched, there is not strict agreement in defining failure criterion and equivalence, interaction in tests representing these two methods that can cause misunderstandings in detecting color vision deficiency (CVD) and gathering statistical reports as well.

For each method we used digitized color vision assessment detecting test. Each test consisted of 16 sequentially chosen stimuli with each sequence performed in three different levels of saturation starting with the most saturated. Sorting method was examined first with participant instructed to arrange stimuli in the given circle starting from the given test cap. And with instructions to choose cap that is the closest match to centered reference color participant was tested with forced choice method next.

We analyzed our results with moment of inertia method that is based on quantifying the angle of alignment of color difference confusion axis and defining CVD severity.[1] **References** 

[1] Vingrys, A.J., and Smith, E.K., A Quantitative Scoring Technique for Panel Tests of Color Vision. Investigative Ophthalmology and Visual Science **29(1)**, 50-63 (1988)

### Spatial speeded verification test in condition of mental fatigue

Elina Vevere<sup>1\*</sup>, Jurgis Skilters<sup>2</sup>, Vsevolod Liakhovetckii<sup>1,3</sup>, Gunta Krumina<sup>1</sup>

<sup>1</sup>University of Latvia, Department of Optometry and Vision Science, Riga, Latvia

<sup>2</sup>University of Latvia, Center for the Cognitive Sciences and Semantics, Riga, Latvia

<sup>2</sup>Pavlov Institute of Physiology, Russian Academy of Sciences, St.Petersburg, Russia

\*E-mail: elina-vevere@inbox.lv

#### Introduction

Mental fatigue is a condition caused by a prolonged performance of a cognitive task. This condition is characterized by subjective feelings like tiredness and lack of energy  $(Johansson\&R\"{o}nnb\ddot{a}ck,~2012)$ . Our research aim is to determine how mental fatigue affects human visuospatial perception and how it is reflected in response times.

#### Method

The research included 74 participants (ages 18-35). Participant's task was to give the fastest possible response time whether a statement corresponds with an image. The statement contained two prepositions - above and below. Participants had to assess 192 combinations of the statement and image. At the end they had to provide answers on a questionnaire concerning their subjective fatigue, health and demographic details.

#### Results

When statement ("true") and the layout of objects match each other, participant gives a faster response  $(0.95\pm0.02~s)$  than if the statement does not coincide with the picture  $(1.11\pm0.02~s)$ . The use of prepositions "above" and "below" has an effect on response times as well – in case of "below" it is longer  $(1.00\pm0.04~s)$  than "above"  $(0.90\pm0.03~s)$ . Unexplained remains the difference between prepositions "above" and "below" statistically significant difference in response time and the number of errors. If the effects of fatigue on the response time and errors considered, then a strong correlation cannot be observed. Longer reaction time is in the morning (although fewer errors are done  $(1.09\pm0.02~s)$ ). During the day people are faster in matching statement with image, but the number of errors tends to increase.

#### Conclusion

It seems to be easier to perceive the statement and image matching and contrary. It seems to be more difficult to perceive and accept a negation (where research participants spent more time on matching sentence and picture).

#### References

*Johansson*, *B.*, & *Rönnbäck*, *L.* (2012). Mental Fatigue; A Common Long Term Consequence After a Brain Injury, Brain Injury - Functional Aspects, Rehabilitation and Prevention, Prof. Amit Agrawal (Ed.), ISBN: 978-953-51-0121-5, InTech, DOI: 10.5772/27042.

#### Changes of blur sensitivity during the day

Anete Petrova\*, Laura Strautina, Peteris Cikmacs
Department of Optometry and Vision Science, University of Latvia, Jelgavas 1, Riga, Latvia,
LV-1004

\*E-mail: anete.petrova@lu.lv

It is shown that blur sensitivity thresholds increase after blur adaptation [1,2]. The aim of this study was to find out if near visual load during the day will cause change in just noticeable blur and clear image perception threshold. These subjective blur perception thresholds were evaluated in group of 12 participants before and after 5 hour long visual load at near distance. Blur was simulated using Gaussian low pass filter. Landolt rings of 3 different sizes (5, 7 and 10 min of arc) were used as stimuli.

Results showed that just noticeable blur threshold increased during the day. Using the smallest stimulus (5 min of arc) just noticeable threshold increased on average by 56% (p = 0,002). Using medium size stimulus (7 min of arc) threshold increased on average by 21% (p = 0,018), but using the largest stimulus (10 min of arc) threshold was on average by 23% (p = 0,019) higher in afternoon session than in the morning session.

- [1] Cufflin MP, Manowska A, Mallen EAH, Invest Ophthalmol Vis Sci. **48**, 2932-2939 (2007)
- [2] Wang B, Ciuffreda KJ, Vasudevan B, Vision Reseach **46**, 3634-3641 (2006)

### Changes in physiological astigmatism with accommodation in emmetropes

Karola Panke<sup>1\*</sup>, Aiga Svede<sup>1</sup>, Wolfgang Jaschinski<sup>2</sup>, Gunta Krumina<sup>1</sup>

<sup>1</sup>Department of Optometry and Vision Science, University of Latvia, Jelgavas 1, Riga

<sup>2</sup>2Leibniz Research Centre for Working Environment and Human Factors (IfaDo), Research

Group "Individual Visual Performance", Dortmund, Germany

\*E-mail: karola.panke@inbox.lv

**Introduction:** Most young emmetrope eyes are far from ideal and have some degree of minor spherocylindrical error including also physiological astigmatism. Because of the changes in the shape of optical interfaces, pupil size, eyelid pressure, tear film, body posture, binocularity and accommodation astigmatism is considered as constantly dynamic phenomenon [1]. The purpose of this study was to evaluate and quantify changes in physiological astigmatism with accommodation.

**Method:** Twenty young emmetropes with mean age  $24 \pm 4$  years and with mean objective refraction within the range of  $\pm$  0.5 D for both spherical and cylindrical power (SE 0.11  $\pm$  0.26 D) were selected for the study. Refraction and accommodative response were measured monocularly for dominant eye with an open-field infrared autorefractometer (Shin-Nippon, SRW-5000) at far (7 m) and near (30 cm). Each measurement consisted of approximately 130 dynamic data points collected during consecutive 2 min time.

**Results:** Clinically and statistically significant increase in cylindrical power and change in cylindrical axis with accommodation (stimulus demand 3.33 D) was seen in 80 % of participants presenting average change of  $0.22 \pm 0.10$  D for power and  $37 \pm 7^{\circ}$  for axis (paired t-test: p=0.001). Changes in a direction towards with-the-rule astigmatism was observed in 56 % of participants, while changes towards against-the-rule direction for 44 %. Our results are only partially in an agreement with previous studies that has observed astigmatism changes with accommodation towards with-the-rule direction [2, 3]. Our results suggest that direction of astigmatism change might be related to baseline astigmatism. For 75 % of participants changes occurred towards closest principal meridian.

**Conclusions:** Results are in a good agreement with previous studies that has found that power of astigmatism increase with accommodation. As regards to the direction of the change of astigmatism our results suggest that it is related to baseline astigmatism and will change towards closest principal meridian.

- [1] Mohammadi, S. F., et al., Physiology of Astignatism, Physiology and Management (2012)
- [2] Cheng,H.,et al.,A population study on changes in wave aberrations with accomodation,J Vi4-4,272-80(2004)
- [3] Tsukamoto,M.,et al.,Accommodation causes with-the-rule astigmatism in emmetropes,Optom Vis Sci77-3,150-155 (2004)

### Pupil diameter changes within mental rotation task under fatigue conditions

Julija Tomilova<sup>1\*</sup>, Jurgis Skilters<sup>2</sup>, Vsevolod Liakhovetckii<sup>3</sup>, Gunta Krumina<sup>1</sup>

<sup>3</sup>Pavlov Institute of Physiology, Russian Academy of Sciences, St.Petersburg, Russia \*E-mail: julijatomilova@gmail.com,

Mental fatigue causes inability to qualitatively perform cognitive tasks that require self-motivation and attention. The pupillary constriction together with higher oscillations is observed for tired person. This is due to the fact, that the more person fells fatigue, the higher is oscillations frequency and range[1]. Mental rotation is the spatial perception of the ability to understand how the object will look like after its rotation through a certain angle [2]. As this task requires constant attention, it is suitable to check the growing mental load on human mental performance. Noreika with colleagues (2013) stated that during the long-term mental rotation test performance there is a significant increase in subjective endpoint fatigue. In addition to this, there are changes in cardiac parameters (heartbeat decreases)[3]. The aim of this research is to assess whether changes in pupil diameter can be used as objective fatigue measure of assessing spatial perception ability.

In order to assess the mental rotation ability the computerized test was created based on Shepard and Metzler research (1971) [2]. 256 pair figures (2D and 3D) were shown to the participants of the research, which were turned  $0^{\circ}$ ,  $60^{\circ}$ ,  $120^{\circ}$ , 180 degree relative to each another. When the pair of figures is shown on screen the participants have to assess if presented figures are similar, but rotated or figures are mirror images of each other. The test will be repeated several times in a row. Among tests, participants have to evaluate subjective fatigue using Licert scale (from -2 to +2), daily regimen. Objective fatigue assessment is carried out in pupil diameter monitoring with the use of SMI RED500 binocular eye movement equipment.

Tendency of pupil's constriction can be observed during the test after the first measurements. Minimum pupil diameter during first test results has shown 6.5mm, after the second it was - 5.8mm (in the dark). In the end of the second test the frequency of blinking has increased. It is not yet enough data to be able to judge the overall trends that may change pupillary constriction and blink increases.

- [1] Lowenstein, O., Feinberg R, Loewenfeld I.E., Pupillary movements during acute and chronic fatigue. *Investigative Ophtalmology*, **2(2)**, 1-18, (1963)
- [2] Shepard, R., Metzler, J., Mental rotation of three-dimensional objects. *Science*, **117**, 701-703, (1971)
- [3] Noreika, D. et al., Interaction of practice and fatigue effects in mental rotation. *Conference "Biomedical Engineering"*, **17(1)**, 97-100, (2013)

<sup>&</sup>lt;sup>1</sup>University of Latvia, Department of Optometry and Vision Science, Riga, Latvia, LV-1063 <sup>2</sup>University of Latvia, Center for the Cognitive Sciences and Semantics, Lomonosova 1A, Riga, Latvia, LV-1019

### The possibility of using NnO NPs as a transducer for optical biosensor for the blv leucosis detection

Shavanova K.<sup>1,\*</sup>, Ruban Yu.<sup>1</sup>, Shpyrka N.<sup>1,\*</sup>, Starodub N.<sup>1</sup>, Khranovskyy V.<sup>1</sup>

<sup>1</sup>National University of Life and Environmental Sciences of Ukraine Heroyiv Oborony st., 15,

Kyiv-03041, Ukraine.

<sup>2</sup>Department of Physics, Chemistry and Biology (IFM) Linköping University \*E-mail: shavanova@gmail.com,

In this paper we demonstrate the possibility of using ZnO NPs as a transducer for the BLV Leucosis biosensors. Sensing capacity ZnO NPs is delivered by the change of UV photoluminescence signal from nanoparticles upon increase of Antiserum BLV concentration in the solution.

Bovine leukemia virus (BLV) is a retrovirus closely related to the human T-lymphotropic virus type 1 HTLV-I. That virus can cause significant economic losses by it decreasing milk and meat quality. In last one particularly, direct band gap semiconductor materials, such as ZnO nanoparticles, usually demonstrate intense and bright luminescence of excitonic type. That's why they are promising as a transducer material and can grant number of benefits for biosensors.

The goal of our work was development of novel type of optical label-free biosensors for detection BLV and their application in food monitoring. The PL intensity was demonstrated to decrease in an exponential fashion with decrease antigen-antibody complex concentration. The obtained results shown that ZnO NP can be used in further experiments for creation novel optical biosensors.

## Estimation of the effect of radionuclide contamination on vicia sativa l. cfi parameters using "floratest" optical biosensor

Ruban Yu.<sup>1</sup>, Illienko V.<sup>1</sup>, Pareniuk O.<sup>2</sup>, <u>Shavanova K.</u><sup>1,\*</sup>

<sup>1</sup>National University of Life and Environmental Sciences of Ukraine Heroyiv Oborony st., 15,

Kyiv-03041, Ukraine

<sup>2</sup> Institute of Environmental Radioactivity of Fukushima University \*E-mail: shavanova@gmail.com

The following article describes the results of testing the sensitivity of Vicia sativa L. to stress factors like radionuclides contamination, using "Floratest" fluorometer. The chlorophyll induction of fluorescence method is showing the integral photosynthesis intensity and the state of plants' photosynthetic membranes. Presented research aimed to determine the parameters of chlorophyll fluorescence induction curve for vetch plants. Seeds of Vicia sativa L. were inoculated by 5 species of potentially radionuclide-blocking bacteria (Agrobacterium radiobacter IMB B-7246, Azotobacter chroococcum UKM B-6082, A. chroococcum UKM B-6003, Bacillus megaterium UKM B-5724, Rhizobium leguminosarum bv. viceae) and grown in sod-podzolic, chernozem, peat-bog soils, contaminated with 137Cs ( $4000\pm340~\text{Bq/kg}$ ). In accordance with our results, combination of soil radionuclide contamination and presence of B. megaterium UKM B-5724 is the most stressful for vetch plants, as the number of inactive chlorophyll increased. Other bacteria showed radioprotective properties in almost all types of soil.

### Control of patulin by immune biosensor based on the structured nano-porouse silicon

Shpyrka N., Shavanova K.<sup>1,\*</sup>, Starodub N<sup>1</sup>,

<sup>1</sup>National University of Life and Environmental Sciences of Ukraine Heroyiv Oborony st., 15, Kyiv-03041, Ukraine.

\*E-mail: shavanova@gmail.com,

The efficiency of the nano-porous silicon (sNPS) application as the transducer in the optical immune biosensor designed for the control of mycotoxins level in environmental objects was studied. Patulin was chosen as model object.

Boron doped single-crystal silicon square wafers with the resistivity of 1 Ohm\*cm, area of  $100~\text{cm}^2$  and thickness of 0.3~m was used. The surface was prepared by stain etching in 4HF:1HNO3:4H<sub>2</sub>O solution. sNPS surface is regularly covered with nano-scale hills up to 20 nm high. The registration of the specific signal was made on the basis of changes of photocurrent of the sNPS.

The biosensor sensitivity for both variants was 10 ng/ml at with the total time of analysis 40 min. This time may be a sharp decline if specific antibodies (Ab) will be preliminary immobilized. It was concluded that the proposed immune biosensor was effective in case the analysis is performed in screening regime. The obtained calibration curves with the model solution of patulin open perspective for the practical application of the proposed immune biosensor in case of the determination of others micotoxins and also others types of toxic substances with the use of their specific Ab.

#### Evaluation of effective area of ytterbium doped optical fiber

Ingrida Lavrinovica<sup>1</sup>, Jurgis Porins<sup>1</sup>, Andis Supe<sup>1</sup>

<sup>1</sup>Institute of Telecommunications,Riga Technical University, Azenes st.12, Riga, Latvia, LV-1048

 $^*\textit{E-mail}:$ ingrida.lavrinovica\_1@rtu.lv

The usage of ytterbium doped fibers is one of the most attractive solutions to increase an output power of optical amplifiers as it ensures low non-linearity, without affecting the amplification efficiency. Yb provides strong absorption in the 820 nm to 830 nm region, where pump excited state absorption (ESA) is significantly smaller, but where ground-state absorption (GSA) is strong enough.

In this research an effective area of ytterbium doped fiber is measured experimentally by interferometric method for different fiber lengths. The effective area value is important at defining the nonlinear effects in a fiber; therefore, it is useful to obtain this value for a particular optical fiber with definite optical transmission parameters.

Based on experimental results the fiber effective area  $A_{\text{eff}}$  has been calculated for different length of ytterbium doped fibers. Usually this parameter is not specified by the manufacturer of optical fiber so mentioned experiment gives a significant benefit for further research in development of optimal ytterbium-doped optical amplifier (YDFA) configuration.

- [1] Porins J., Supe A., Bobrovs V., Evaluation of Effective area in Erbium Doped Fibers, Lithuanian Journal of Physics, Vol. 52, No. 1, pp. 19–23, (2012).
- [2] Bobrovs V., Ivanovs G., Parameter Evaluation of a Dense Optical Network// Electronics and Electrical Engineering, No .4, pp. 33-36. (2006).

### Device for retinal illumination and circadian light monitoring

<u>Kalvis Kundrats</u><sup>1</sup>, Sergejs Fomins<sup>2,\*</sup>, Maris Ozolinsh<sup>2</sup>

<sup>1</sup>Optometry and Vision Science Dept., University of Latvia, Jelgavas 1, Riga, Latvia, LV-1001 <sup>2</sup>Institute of Solid State Physics, University of Latvia, Kengaraga 8, Riga, Latvia, LV-1063 \*E-mail: sf00017@lu.lv

Since the action spectrum of human circadian system is known [1, 2], it is possible to measure the amount of photons potentially absorbed by the circadian system. The device for characterization of the light in terms of non-object forming vision circadian system  $C(\lambda)$  being introduced about ten years ago [3].

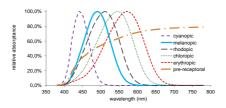


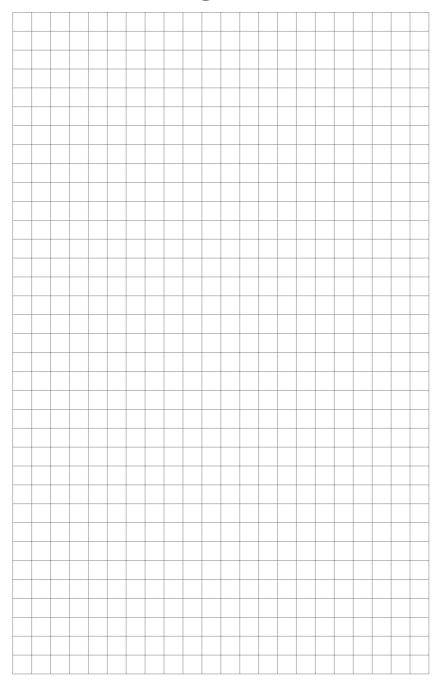
Figure 13: Receptor sensitivities and pre-receptor filter. Solid curve represents the melanopic action spectrum [4].

Existing method provide data not related to the retinal illumination controlled by the eye's pupil. Spatial scene structure in the field of view of the subject could also impact the size of pupil. Therefore, we propose a system for eye pupil tracking in parallel to acquisition of visual scene and circadian light.

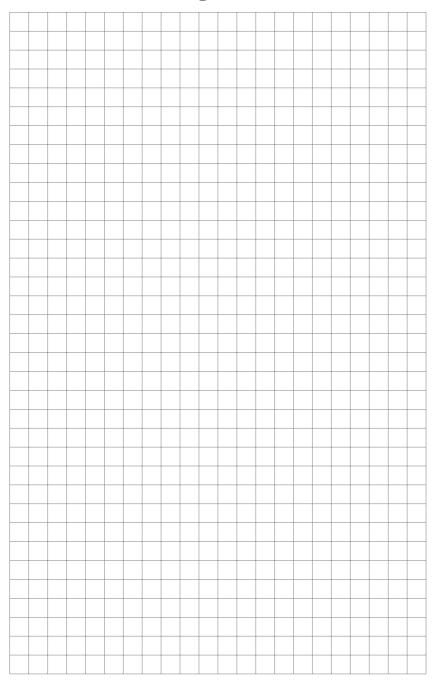
The lightweight system is based on the spectacle frame and is equipped with calibrated sensors for photometric and circadian light measurements. Eye's pupil data is measured by near infrared micro camera. Data processing and storage, adaptive control of NIR illumination and camera sensitivity is provided by microcomputer. Second RGB large angle camera provides the low resolution QVGA scene data stored in 4 bit dynamic depth. Developed device allows everyday measurements of the scene data and subject eye pupil on the continuous basis for 4 hours at the moment. We propose the system for long-term analysis of pupil reflex changes in relation to environment illumination characteristics.

- [1] Rea et al., Brain Res Rev 50, 213-228 (2005)
- [2] Bailes et al., Proc R Soc B. 280, 20122987 (2013)
- [3] Gall et al., Proc CIE symposium'04, 129-132, Vienna, Austria, (2004)
- [4] CIE TN 003:2015

### Notes – DOC 2016, Riga, March 21-23, 2016



### Notes – DOC 2016, Riga, March 21-23, 2016



#### DOC 2016 is Organized and Supported by:

# OSA University of Latvia Student Chapter

# SPIE STUDENT CHAPTER UNIVERSITY OF LATVIA

















